



THE UNIVERSITY *of* EDINBURGH

Edinburgh Research Explorer

Natural Algae-Inspired Microrobots for Emerging Biomedical Applications and Beyond

Citation for published version:

Li, Z, Liu, T, Sun, X, Zhou, Q & Yan, X 2024, 'Natural Algae-Inspired Microrobots for Emerging Biomedical Applications and Beyond', *Cell Reports Physical Science*, vol. 5, no. 6, 101979.
<https://doi.org/10.1016/j.xcrp.2024.101979>

Digital Object Identifier (DOI):

[10.1016/j.xcrp.2024.101979](https://doi.org/10.1016/j.xcrp.2024.101979)

Link:

[Link to publication record in Edinburgh Research Explorer](#)

Document Version:

Peer reviewed version

Published In:

Cell Reports Physical Science

General rights

Copyright for the publications made accessible via the Edinburgh Research Explorer is retained by the author(s) and / or other copyright owners and it is a condition of accessing these publications that users recognise and abide by the legal requirements associated with these rights.

Take down policy

The University of Edinburgh has made every reasonable effort to ensure that Edinburgh Research Explorer content complies with UK legislation. If you believe that the public display of this file breaches copyright please contact openaccess@ed.ac.uk providing details, and we will remove access to the work immediately and investigate your claim.



Natural Algae-Inspired Microrobots for Emerging Biomedical Applications and Beyond

Ziqiao Li^{1,†}, Ting Liu^{1,†}, Xiang Sun¹, Qi Zhou^{2,**}, Xiaohui Yan^{1,3*}

¹State Key Laboratory of Vaccines for Infectious Diseases, Center for Molecular Imaging and Translational Medicine, Xiang An Biomedicine Laboratory, School of Public Health, Xiamen University, Xiamen 361005, China.

²School of Engineering, The University of Edinburgh, Edinburgh EH9 3FB, United Kingdom.

³Shenzhen Research Institute of Xiamen University, Shenzhen 518057, China.

Correspondence: **q.zhou@ed.ac.uk (Q. Z.); *xhyan@xmu.edu.cn (X. Y.)

[†]These authors contributed equally to this work

Summary

Algae-inspired microrobots (AIMs) have attracted intense research over the past decade owing to the abundant desired properties of natural microalgae, such as biocompatibility, autofluorescence, and pharmaceutical activity, which make them ideal candidates for biomedical and related applications. With the deepening and widening of applied research, the functions of AIMs have been greatly enriched and enhanced to meet the needs of demanding application scenarios including targeted drug delivery, anticancer/antibacterial therapy, cell stimulation, wound healing, biomolecule sensing, etc. Notwithstanding, multiple challenges remain to be tackled for transformative advances and clinical translation. In this review, we aim to provide a comprehensive survey of representative advances in AIMs accompanied by the underlying biological/technological backgrounds. We also highlight existing issues that need to be overcome in future AIM developments and suggest the directions of future research in this field.

Keywords

Micro/nanorobots, Biological motors, Bio-inspired actuators, Targeted delivery, Nanomedicine, Anticancer/antibacterial therapy, Biomolecule detection, Cell stimulation, Enzyme catalysis

INTRODUCTION

Micro-/nanorobots are miniaturized motors that can be actuated using fuel-driven (*e.g.*, hydrogen peroxide, acid, bromine, and iodine)¹⁻³ or fuel-free driving methods (*e.g.*, electrical, ultrasound, light, and magnetic fields).⁴ In recent years, they have demonstrated superior ability for overcoming biological barriers with precise navigation to hard-to-reach tissues/cavities (some inaccessible to conventional approaches) and are therefore envisioned for advanced biomedical applications such as targeted drug delivery, minimally-invasive surgery, detoxification, biosensing, and so on.⁵⁻⁹ Notwithstanding, critical challenges still persist for further development of the technology toward clinical translation, primarily arising from the integration and optimization of multiple functions onto biosafe micro-/nanorobots while ensuring the ease of fabrication in bulk at low costs.

Nature provides a wealth of solutions to scientific questions and has indeed inspired novel designs of micro-/nanorobots. One example is from microorganisms in nature, which have gone through centuries of natural selection to evolve diverse structures and functions, *e.g.*, hydrophobicity/hydrophilicity, biodegradability, magnetotaxis, and autofluorescence.¹⁰⁻¹⁵ Microrobots fabricated through modifying natural microorganisms with engineered components can perform highly specific tasks, for which the desired functionality of the microrobots is either intrinsically endowed by properties of the host microorganisms or synthetically enabled by functionalization of the microorganisms through structural design, surface modification, cargo-loading, etc.¹⁶⁻²⁰ Because a variety of microorganisms are freely available in nature and can be

conveniently cultured under laboratory conditions, cost-effective mass production of micro-/nanorobots for population-level applications through this route is feasible.

As a subset of microorganisms, microalgae have been widely studied and commercialized owing to their abundance of bioactive compounds, equipping them with intriguing features such as phototactic property, pharmaceutical activity, and high-quality nutrients. Furthermore, compared with other microorganisms which may also have some of the above features (e.g., bacteria and paramecia), microalgae are in general free of cytotoxicity concerns and capable of photosynthesis too, making them desirable for food supplements and biomedical exploitations. Accommodating these desired functions in a body size of dozens of micrometers provides useful options for the engineering of algae-inspired microrobots (AIMs).¹⁸⁻²⁰ Dating back to 2005, the earliest prototype of AIM “microoxen” was demonstrated using *Chlamydomonas reinhardtii*²¹ (**CR**, a model organism in labs; see Fig. 1a) as biological motors to transport microparticles with high efficiency.²² To date, a range of microalga species of distinct morphologies, including *Volvox* (**VX**; Fig. 1b),²³ *Eudorina elegans* (**EE**; Fig. 1c),²⁴ *Pandorina morum* (**PM**; Fig. 1d),²⁵ *Chlorella* (**Ch**; Fig. 1e),²⁶ *Spirulina platensis* (**SP**; Fig. 1f),²⁷ *Diatom* (**DM**; Fig. 1g),²⁸ and *Tetraselmis subcordiformis* (**TS**; Fig. 1h),²⁹ have been explored by researchers to engineer AIMs for emerging biomedical applications and beyond (Fig. 1i; more examples listed in Table 1).^{21-25, 30-44}

Compared with conventional medical tools in clinics, AIMs are capable of precisely delivering therapeutic cargoes to targeted positions and then releasing them in a controlled manner for on-demand tasks (e.g., antibacterial/anticancer therapy) in biofluidic environments, therefore minimizing the drug dosage and associated adverse effects on normal cells.^{26, 33, 39, 44} Specific functions can also be integrated into AIMs to enable challenging operations at the single-cell level, such as controlling neural-cell differentiation and inducing muscle-fiber contraction.^{45, 46} One particular advantage of AIMs over other types of micro-/nanorobots (e.g., catalytic micromotors relying on toxic fuels and ferromagnetic microrobots made of cytotoxic materials like NeFeB) is their natural biocompatibility and desired biodegradation that helps bridge the overwhelming biosafety gap between current micro-/nanorobotic research and clinical translation, envisioning for accelerated biomedical applications benefiting patients in need. Apart from biomedical applications, AIMs have also been explored for remote sensing,²⁸ on-cell catalysis,³⁶ and environmental remediation,⁴⁰ manifesting the breadth of their potential in resolving real-world issues. Given the wide commercialization of microalgae products in the agriculture and healthcare sectors, the prospects for continued development and maturation of AIMs toward practical bench-to-bed translation are promising.

In this review, we systematically review recent progress in the fabrication, control, and applications of common AIMs, aimed at informing an atlas of microalgae functionalization and application strategies to accelerate the development of versatile AIMs toward practical applications in clinics. We also discuss the strengths and weaknesses of existing AIMs and provide an outlook for future research directions, including functionality expansion of existing AIMs, inception of new types of AIMs, and innovation of advanced control systems for widening and deepening applications of AIMs in biomedicine and beyond. The scientific rationale, technological basis and cost-effectiveness for pursuing advanced biomedical applications using microalgae-based biorobotics have been introduced in detail by recent reviews,⁴⁷⁻⁵¹ and the readers are referred to these works for a broader understanding of the emerging research field.

CLASSIFICATION OF ALGAE-INSPIRED MICROROBOTS (AIMS)

AIMs can be divided into three categories based on whether they retain the microalgae cell activity and whether they preserve the original biological substrate: microalgae-flagellated robots (MFRs), microalgae-hybrid robots (MHRs), and microalgae-templated robots (MTRs).

MFRs are defined as living microalgae deployed as motile microrobots, usually subject to surface decoration with other structures/molecules. Such microalgae usually come with beating

100 flagella, endowing superior propulsion and sensing capabilities to the as-fabricated microrobots.⁵²
101 Their flagella are capable of efficiently converting chemical energy into mechanical work through
102 molecular motors powered by adenosine triphosphate (ATP) hydrolysis. These microalgae have
103 desired features like phototaxis,⁵³ chemotaxis,⁵⁴ and/or electrotaxis,⁵⁵ which provide steering
104 mechanisms for motion control. MFRs have been developed for wide-ranging applications, *e.g.*,
105 thrombus clearance,⁹ cargo delivery,⁴³ and environmental remediation.^{40, 56} Certain nutrient
106 environments are usually required to ensure the controlled functioning of MFRs, which would
107 otherwise experience flagella inactivation and loss of motility. It is also important to consider their
108 maintained activity and steerability for monitored operations, especially in deep tissues.

109 MHRs are defined as non-living biohybrid microalgae with optional functional modifications
110 on the algal surface or within the cells. The morphological structure and biological substances of
111 the microalgae will be preserved, but the cell activity is forfeited. With externally coated materials,
112 mostly common magnetic substances like Fe₃O₄ nanoparticles (NPs), it is possible to confer
113 magnetic attributes to the microalgae for remote actuation and steering using magnetic fields.
114 MHRs are versatile in varying scenarios because they can perform complex tasks even in harsh and
115 toxic environments. Additionally, the biological compounds inherited from the microalgae cells
116 can equip MHRs with desired functionalities such as autofluorescence, magnetic resonance (MR)
117 signals, and anticancer activity.³³ Through further integration of additional components, other
118 functions such as photoacoustic (PA) imaging and antibacterial therapy can be achieved, enabled
119 by polydopamine (PDA).⁵⁷ Benefiting from diverse functionalization strategies, MHRs can be
120 customized to accommodate a plethora of functions in a single package suiting their applications.
121 When choosing the chemical composition of MHRs for *in vivo* applications, crucial aspects
122 including cytotoxicity, biodegradation, imaging capability and potential immune responses should
123 be considered.

124 MTRs are defined as synthetic microrobots merely replicating the microalgae morphology,
125 with both the structural matrix and contained compounds removed after fabrication.^{31, 41} MTRs rely
126 on an electrochemical deposition-like process in the sense that the microalgae mainly provide a
127 biological template for shaping the microrobots, regardless of their cellular activity and intrinsic
128 functionalities, which are eventually eliminated. Owing to the internal cavity space freed during the
129 fabrication procedures (*e.g.*, annealing treatment), a large quantity of macromolecules or drug
130 payloads can be loaded in MTRs for targeted delivery and controlled release. During the fabrication
131 process, the microalgae structure is susceptible to excessive damage, potentially affecting the
132 locomotion performance of MTRs. Therefore, factors such as temperature and reaction time need
133 to be precisely controlled to preserve the desired microalgae morphology.

135 MANUFACTURING METHODS

136 Microalgae-flagellated robots (MFRs)

137 For fabricating MFRs, there are primarily two requirements for the microalgae candidates. First,
138 they should be able to swim in fluid environments or glide on surfaces, with continuous propulsive
139 forces generated to empower their locomotion. Second, they need to demonstrate a certain tropism
140 for controllable steering of motion toward target locations. Microalgae with flagella or cilia, mostly
141 green algae (*e.g.*, *CR*, *Volvox*, *EE*, *PM*), can intrinsically act as MFRs. For instance, through the
142 phototaxis of *CR* and *EE*, a novel guiding system was developed for guiding them to traverse
143 crossing channels and transport microscale loads.²⁴ Similarly, transport of submillimeter-sized
144 cargo has been demonstrated using *Volvox*.³⁷ *CR* and *PM* were exploited as bio-tweezer systems to
145 manipulate micro-objects,²⁵ with their performance evaluated considering both hydrodynamics and
146 Brownian motion. Without advanced functional modifications, MFRs in the above studies were
147 mostly suited for relatively simple tasks.

148 To enable MFRs for designated functionalities, various strategies to modify the microalgae
149 surface with exogenous materials have been proposed. For example, polystyrene (PS) beads

150 decorated with synthetic 4-hydroxyproline (4-HP) polypeptides were loaded onto the outer surface
151 of *CR* (which is primarily composed of 4-HP-rich glycopeptides) through noncovalent
152 interactions,^{22, 58} with the size and number of loaded PS beads controlled by adjusting their relative
153 concentration to that of *CR* samples. The noncovalent method was also utilized for reversibly
154 anchoring antibiotic vancomycin (Fig. 2a).⁵⁹ Electrostatic adsorption, relying on the negative charge
155 of the microalgae cell wall or membrane to deposit positively charged materials, is a widely applied
156 noncovalent method for MFRs (Fig. 2b-d). For instance, chitosan polymer could be attached to the
157 microalgae surface^{21, 23} for accommodating biomedical cargo molecules. Santomauro *et al.*
158 proposed MFR magnetization by terbium,⁶⁰ which were absorbed onto the algae cell wall due to
159 electrostatic interaction. Negatively charged microbeads could also be converted into positively
160 charged for further electrostatic interaction with the microalgae cell wall, through modification with
161 cationic poly(diallyldimethylammonium chloride) (PDDA),⁶¹ or layer-by-layer deposition of
162 polyelectrolytes PAH/PSS.³⁴ Typically, noncovalent binding is a simple method with minimal
163 damage to the algal cells, but it suffers from instability and uncertainty.

164 On the other hand, covalent modification methods have been exploited given their stable
165 bonding. One example was Szponarski *et al.*,³⁶ where the cell wall of *CR* was decorated with
166 artificial metalloenzyme *via* specific binding of biotin to streptavidin through the reaction of the
167 amino acid residues bearing amino groups with electrophiles such as N-hydroxysuccinimide esters
168 (Fig. 2e). Biorthogonal click chemistry was also introduced to functionalize *CR* with NHS-
169 dibenzocyclooctyne anchor (DBCO), which allowed an azide derivative of the drug to be bonded
170 to the surface (Fig. 2f).^{62, 63} Similarly, *CR* was functionalized by angiotensin-converting enzyme 2
171 (ACE2) receptor and antibiotic-loaded neutrophil membrane-coated polymeric NPs to remove
172 SARS-CoV-2 spike proteins from aquatic media^{40, 56} and to treat acute bacterial pneumonia,⁴²
173 respectively.

174 **Microalgae-hybrid robots (MHRs)**

175 MHRs have been fabricated mainly using *SP*, *Ch*, and *Diatom* (occasionally with *CR* and *TS*), which
176 are actuated and controlled by externally applied magnetic fields. Several methods have been
177 employed to magnetize the microalgae, such as dip-coating, electroless deposition/plating, and
178 physical vapor deposition, followed by post-modification functionalities added for designated
179 applications (Fig. 3). Using a facile dip-coating process in Fe₃O₄ NP suspensions, Yan *et al.*
180 developed a multifunctional MHR from *SP* (*CR* and *TS* MHR fabricated too) with intrinsic
181 properties of autofluorescence, biodegradation, and selective cancer-cell cytotoxicity.³³ The
182 superparamagnetic magnetite NPs not only enable magnetic response and magnetic resonance
183 signals for the MHR, but also provide a versatile base for multi-purpose functionalization. To
184 enhance the propulsion efficiency of MHR, Gong *et al.* deposited nickel (Ni) coating onto the
185 surface of *SP* through an electroless plating technique,³⁵ which achieved a propulsion velocity up
186 to 2613.8 μm/s (about 12 body lengths per second) compared to the Fe₃O₄ NP dip-coated MHRs
187 (average velocity *ca.* 90 μm/s). The swimming performance of Ni-coated diatomite microswimmer
188 under a rotating magnetic field was also characterized by the same group.⁶⁴ On the other hand side,
189 electron-beam physical vapor deposition was applied by Guo *et al.* for depositing Ni and Au film
190 on one side of the *Diatom* frustules, and synthesized Ag NPs were uniformly distributed on the
191 surface for SERS detection.²⁸

192 Depending on the target functions for a designated application, the post-modification process
193 can be either directly implemented on the MHRs or through additionally introduced functional
194 substances. Thanks to the porous structure of MHRs, biomacromolecules and small molecules can
195 be encapsulated *via* a simple osmotic diffusion or dehydration/rehydration process of the
196 microalgae cells, which serves as a promising approach for drug loading and targeted delivery.³⁸
197 As for exogenous functional substances, PDA (given its strong NIR adsorption and high
198 fluorescence quenching properties) has been coated on MHRs to endow them with photoacoustic
199

(PA) imaging and photothermal effects,⁵⁷ which could also be acquired by loading Pd@Au or CuS NPs in algae cells by electroless deposition.^{27, 65} One promising advance is to combine chemotherapeutic drugs with the photothermal effect of MHRs, which can realize dual-model therapy of cancer cells.²⁷ Another prospect is to modulate tumor hypoxia and release reactive oxygen species through radiotherapy treatment of magnetite-coated microalgae for multimodal tumor inhibition.³⁰ Apart from anticancer and tumor therapy, magnetic MHRs post-modified with BaTiO₃ NPs through electrostatic adsorption have demonstrated the ability to control the differentiation at the single-cell level.^{45, 66}

Microalgae-templated robots (MTRs)

Owing to the abundance of microalgae structures in nature, MTRs with various shape options can be conceptualized and fabricated. Compared to microrobots designed by computer programs and manufactured through direct laser writing or template-assisted deposition, MTRs using natural microalgae as biological templates circumvent the cumbersome structure-design process and facile mass-production is possible with well-controlled chemistry in a cost-effective manner. In addition, biological substances of potential toxicity contained in the microalgae can be removed during the fabrication process, which adds to the biocompatibility of MTRs while supporting bulk loading of functional cargos for a variety of biomedical applications.

Among others, *SP*-based MTRs have attracted much attention owing to their inherent helical structure conducive to efficient actuation in viscous biofluids. Experimental procedures have been developed for fabricating porous hollow *SP* MTRs with or without a preserved carbon core (Fig. 4a).^{31, 41} In brief, magnetite precursors are first applied to deposit magnetic NPs on the *SP* surface driven by biological extracellular mineralization, during which integrity of the helical structure is maintained throughout. Subsequent annealing treatment (either in vacuum or air) is then employed to remove or transform the *SP* template without altering the deposited coating. Vacuum annealing would result in the acquisition of helical carbon@magnetite core-shell MTRs with the magnetite precursor forming a large quantity of mesopores on the surface, whereas air annealing leads to hematite nanostructured porous hollow micro-helices (Fig. 4b) and further magnetite MTRs after additional reduction reaction. Given the internal cavity structure, MTRs could be exploited to load and release abundant cargos or collect heavy metal ions, serving as a novel platform for the development of biomedical microrobots.

More recently, Diatom frustules have been exploited as naturally porous hierarchical templates to fabricate motorized microsensors²⁸ or cargo carriers.⁶⁷ Guo *et al.* extracted the diatom frustules from diatomaceous earth powders through dispersion, sonification and filtration, followed by high-temperature calcination to clean the organic residues. A magnetic thin film was then deposited using Ni and Au through electron-beam evaporation, after which plasmonic Ag NPs were synthesized on the surface via catalytic reduction of silver nitrate to enable surface-enhanced Raman scattering spectroscopy for bio-detection (Fig. 4c).²⁸ Alternatively, Li *et al.* applied acid treatment to remove the calcareous cementitious substances and internal organic matter of the diatoms (Fig. 4d).⁶⁷ The obtained diatom frustules were then coated with magnetite particles through electrostatic adsorption to facilitate magnetic actuation and control (Fig. 4e).

ACTUATION AND MOTION CONTROL

Similar to living microorganisms and other micro-/nanorobots, AIMs rely on distinct mechanisms from the commonly encountered strokes at the macroscale for effective propulsion of their miniature body.⁵ For AIMs of characteristic length L swimming at a speed of u in a fluid of constant density ρ and dynamic viscosity μ , the Reynolds number (Re) defined as

$$Re = \rho Lu / \mu \quad (1)$$

is far below the order of unity, implying vanishing effect of inertia and instantaneous motion/halt in response to propulsion forces. At this Re limit, any motion of the microrobot that is time-

250 reversible and reciprocal (*i.e.*, periodic, symmetric back-forth strokes) does not lead to net
251 movement, which is known as the “scallop theorem.” There are two common strategies used by
252 living microalgae to break the scallop theorem, namely flagellar beating and helical rotation,^{68, 69}
253 and such propulsion methods can be either directly employed (*e.g.*, for MFRs) or mimicked (*e.g.*,
254 for MHRs and MTRs) by microrobots to achieve locomotion in simple and complex fluid media.⁵

255 Motion control of AIMS, namely real-time steering of their locomotion, is another crucial
256 factor for on-demand operations, and there are two primary categories of approaches widely
257 employed: optical control methods (mainly for MFRs) and magnetic control methods (mainly for
258 MHRs and MTRs). Optical control methods capitalize on the intrinsic light-sensing ability of living
259 microalgae termed as “phototaxis,” where the microalgae demonstrate a tendency of motion toward
260 or against the light gradient. Magnetic control methods rely on the magnetic moment of the
261 magnetic materials (*e.g.*, iron oxide, terbium) integrated on/in the microalgae, based on which
262 magnetic torques or gradient forces are applied to align the magnetized microalgae with the
263 magnetic field direction or gradient direction. In this section, we will discuss in detail the above
264 actuation methods and control methods, together with other available strategies (especially for
265 MFRs) which have also been exploited to achieve designated tasks in complex environments.

266 MFRs

267 As previously introduced in Section 2, the locomotion of MFRs relies on their natural motility
268 through flagellar movements. Flagella are long and thin appendages to the cell body that can
269 perform non-reciprocal strokes or collective motion to generate net displacement under low inertia.
270 As *CR* is the predominant species that has been widely developed as MFRs, we take it as an example
271 to elaborate on the mechanism for flagellum-driven propulsion.

272 *CR* is a unicellular spheroid about 10 μm in dimension with two anterior flagella sprouting
273 from the cell body (Fig. 5a).⁷⁰ The internal motile component within each flagellum is called
274 axoneme (Fig. 5b). The axoneme has a conserved cylindrical architecture consisting of nine outer
275 doublet microtubules and two central microtubules known as the “central pair” (CP), supported by
276 dyneins, radial spokes, nexin for cross-links and regulatory proteins.⁷¹ The dyneins are classified
277 as outer dynein arms providing power output, and inner dynein arms determining the flagellar
278 beating pattern.⁷²⁻⁷⁴ The generated beating motion causes a sliding force between adjacent outer
279 doublet microtubules, which is then converted into bending through the nexin-dynein regulatory
280 complex (N-DRC), a structure interconnecting the outer doublet microtubules and maintaining their
281 alignment. In this manner, dynein efficiently converts the chemical energy *via* ATP hydrolysis into
282 mechanical work. To propel the microalgae body, signals from the CP are transformed through the
283 radial spokes to coordinate the dynein arms for a regular waving pattern and effective propulsion.
284 Axonemes without radial spokes can lead to flagellar paralysis or chaotic beating.^{75, 76} Each
285 beating cycle can be divided into two stages in a breaststroke fashion: power stroke and recovery
286 stroke (Fig. 5c).²² In the former, the flagella flap backward and the cell body moves forward,
287 whereas in the latter the flagella shrink and flap forward pulling the cell body backward to a certain
288 degree. In a full beating cycle, net displacement forward occurs.^{9, 61} Different motion control
289 methods have been developed to steer and direct the MFRs for navigation toward designated
290 positions, including optical control, magnetic field, chemoresponses, and electrotaxis, as to be
291 detailed below.

292
293
294 **Optical control.** Optical control of MFRs usually relies on two approaches: phototaxis and optical
295 tweezers (OT). We take *CR* as an example to explain the first control method, phototaxis. The
296 detection of light by *CR* is through an elaborate subcellular organelle ‘eyespot’ (an orange spot
297 located near the cell equator about 45° ahead of the flagellar beat plane),⁷⁷⁻⁷⁹ containing carotenoid-
298 rich granule layers in the chloroplast and the channelrhodopsin photoreceptor proteins ChR1 and
299 ChR2 in the plasma membrane (Fig. 5d).⁷⁷ With the eyespot, *CR* presents positive phototaxis

300 toward low-intensity light and negative phototaxis against high-intensity light, respectively.
301 Because *CR* rotates its body (about twice a second) when swimming forward, the eyespot scans
302 incoming light from different directions.^{78, 80-82} A photocurrent influx of Ca^{2+} ions into the flagella
303 can be triggered as the eyespot senses the light information,^{83, 84} consequently disrupting the beating
304 balance between the two flagella⁷⁸ and causing the eyespot to tilt toward or against the light source
305 depending on the beat amplitude of either flagellum.⁸² If the swimming path is parallel to the light
306 direction, the eyespot would perceive a constant illumination signal and keep advancing; otherwise,
307 the flagella would realign the cell. This "tracking signal" pattern forms a closed-loop control to
308 steer the cell toward the right direction.⁸⁵ It should be noted that phototaxis is affected by other
309 factors, *e.g.*, the concentration of cations and the temperature of the environment.^{55, 78}

310 In the context of controlled MFR motion using phototaxis, the pioneering work of Weibel *et al.*
311 demonstrated guided transport of microbeads by *CR* cells in a straight channel through their
312 rapid phototactic responses (within 1 s) to the applied LED, with tunable swimming patterns
313 between random, positive, and negative phototaxis under varying light intensities.²² Similarly,
314 Nagai *et al.* achieved unidirectional transport of a submillimeter block using *Volvox* colonies.³⁷ Xie
315 *et al.* developed a novel algae guiding system (AGS) to track and steer *EE* cells along arbitrary
316 trajectories, providing a potential pathway to robotize algae cells for targeted delivery or drug
317 screening.²⁴ Indeed, Shchelik *et al.* realized antibacterial treatment with antibiotics-attached *CR*
318 cells for controlled drug release with robust phototaxis.⁶²

319 The other optical control method widely used for steering MFRs, OT, exerts an optical force
320 on targeted objects with a different refractive index from the surrounding environment. OT is
321 widely used for trapping and manipulation of microparticles or biological materials to measure their
322 physical properties.⁸⁶⁻⁹⁰ The optical force is generated when light interacts with the object, produced
323 by light reflection, absorption, refraction, or scattering due to changes in its momentum.⁸⁹ Xin *et al.*
324 realized controllable locomotion of *CR* cells in a variety of biological media by optical force
325 (Fig. 5e) for indirect manipulation of microparticles and disruption of biological targets such as
326 blood clots.⁹ Furthermore, motor arrays of reconfigurable patterns could be formed by *CR* cells to
327 work independently and collaboratively for different tasks, demonstrating the potential of OT-
328 controlled MFRs as a robotic operation platform with high throughput.⁹

329 Optical control, either through phototaxis or OT, provides extensive opportunities for real-
330 time control of MFRs using light. However, these approaches do have significant limitations. On
331 the one hand, the light signals cannot penetrate sufficient depth in certain environments, and the
332 swimming orientation of MFRs is restricted by the light source position. On the other hand, it can
333 be challenging to integrate a light source into the microscale system and the UV light may cause
334 DNA or protein damage in organisms or humans,^{91, 92} which makes potential biomedical translation
335 difficult. Additionally, the focused light may heat the ambient environment outwith the target zone,
336 therefore causing unintended harm to off-target normal cells.^{6, 18} Therefore, other control methods
337 with desired tissue penetration and biocompatibility are still needed.

338
339 **Magnetic control.** Magnetic fields can wirelessly transmit power with high penetration capacity
340 through the human body in a harmless manner, even with relatively large field strengths.^{5, 6, 93, 94}
341 For MFRs subject to magnetization by magnetic particles,⁶¹ Tb^{3+} ions,⁶⁰ or treated PS microbeads,³⁴
342 a directed magnetic field can be used to control their motion. When exposed to the applied magnetic
343 field, the MFRs would align themselves to the magnetic field direction due to their magnetic
344 moment, thus enabling the steering of MFRs. Indeed, Ng *et al.* and Yasa *et al.* demonstrated that
345 the MFRs showed random helical motion in the absence of magnetic fields, but positive
346 magnetotaxis (artificial) would dominate their motion under low-strength magnetic fields (Fig.
347 5f).^{34, 61}

Chemoresponses. In addition to the optical and magnetic methods introduced above, other strategies have been exploited for controlling the MFRs too, such as chemoresponses.⁵⁴ In general, there are two types of chemoresponses from microalgae. The first is chemotaxis, for which the microalgae respond to chemicals without changing their swimming speed and motility, including positive chemotaxis (associated with algae accumulation) and negative chemotaxis (associated with algae repulsion). The other type of chemoresponses is chemokinesis, where the microalgae accumulate as the chemical stimuli affect their motility (causing reduced or halted swimming of the microalgae). Chemotaxis is a promising control method for MFRs without the need for an external control system, with ideal candidates being those naturally produced in the working media (*e.g.*, chemical signals released by cells can be utilized for eliciting a response). However, some drawbacks do exist, such as the poor spatiotemporal resolution of chemical gradients in the environment and the inevitable response delay that may cause real-time control issues. Furthermore, the orientation control using chemotaxis is also subject to a high degree of stochasticity.^{95, 96}

Electrotaxis. Electric fields have also been applied to navigate MFRs *via* their electrotaxis behavior (galvanotaxis).⁵⁵ One should note the difference between electrotaxis and electrophoresis: the former describes living cells actively swimming toward an electrode in response to electric stimulation, whereas the latter describes objects of net surface charge passively moving under the influence of an electric field.^{19, 97} Hayashi *et al.* showed that *Volvox* would only present negative electrotaxis under a wide range of electric field strengths.⁵⁵ But if photo- and electric-stimulations were coupled, *Volvox* could perform positive electrotaxis, presumably due to cell polarization. As the strength and direction of electric fields can be easily altered, it serves as a feasible control method for MFRs. Nevertheless, electric control methods might be invasive and could induce electroporation of the microalgae cell membranes.⁹⁸ In addition, potential electrolysis may produce toxic gases or change the pH of the working liquid media.^{18, 99}

MHRs and MTRs

External fields, such as electric, magnetic, ultrasound, and light,^{4, 100-102} have been widely exploited for the control of synthetic microrobots. For the actuation and steering of MHRs and MTRs, magnetic fields are the most used, which can enable navigation in complex three-dimensional environments with superior penetration depth and good biocompatibility under a wide range of magnetic field strengths (*e.g.*, the field strength for MR imaging can be as high as 4T under medical supervision).^{5, 6, 93} Typically, an electromagnetic coil system (*e.g.*, tri-axial Helmholtz coils) or permanent magnets are used for generating the magnetic fields needed.¹⁰³ Under a magnetic field \mathbf{B} [T], a microrobot with average magnetization \mathbf{M} [m A^{-1}] experiences a magnetic torque \mathbf{T} [N m] (aligning the microrobot with the magnetic field direction) and a magnetic force \mathbf{F} [N] (pulling or repelling the microrobot along the field gradient direction) given by

$$\mathbf{T} = \vartheta \mathbf{M} \times \mathbf{B}, \quad (2)$$

$$\mathbf{F} = \vartheta (\mathbf{M} \cdot \nabla) \mathbf{B} \quad (3)$$

where ϑ is the volume of the magnetized microrobot.¹⁰³

Both magnetic forces and magnetic torques have been utilized for the actuation of MHRs and MTRs. The magnetic force can be directed to pull the microrobots toward the region of higher magnetic flux density when the field has a gradient, and the pulling force can be enhanced by increasing the gradient of the applied field. Magnetic torques produced by rotating or oscillating magnetic fields, however, are more commonly adopted due to their precision of control, especially for powering helical microrobots that rely on rotation-translation motion (Fig. 6a).³³ The propulsion direction of the microrobots is approximately perpendicular to the plane of the rotating magnetic field, and either forward or backward translation can be achieved by reversing the magnetic field direction.¹⁰⁴ The rotating motion of MHRs and MTRs should ideally be converted into translation synchronously, and there exists a linear relationship between the increase of propulsion velocity

399 and the rotating frequency of the imposed magnetic field within a certain range. However, if the
400 rotating frequency is too high, the magnetic torque may fall short to balance the viscous drag in the
401 swimming environment.¹⁰⁵ In this case, the swimming velocity of the microrobot will actually
402 decrease after reaching a critical rotating frequency known as the “step-out” frequency.
403 Additionally, deviation of the swimming path from the magnetic field direction could happen if the
404 microrobot interacts with surfaces or substrates in the ambient environment when its translation
405 control will be affected. Without the need for any potentially hazardous fuels, magnetic fields
406 remain a popular propulsion method for AIMS, and their extensive applications in various medical
407 settings would be conducive to the clinical translation of AIMS too.¹⁰⁴

408 A large body of research works in the literature have employed rotating or oscillating magnetic
409 fields to steer MHRs and MTRs for controlled navigation.^{27, 31, 33, 35, 38, 41, 45, 57, 64, 66} For
410 magnetization purpose, robust magnetic materials such as Fe₃O₄ and Nickel particles could be
411 deposited on the microalgae, so actuation and steering becomes possible with low-strength
412 magnetic fields for on-demand tasks. Microrobots magnetized from microalgae of various shapes,
413 such as helical and spherical/ellipsoidal ones, have been successfully propelled using magnetic
414 fields (Fig. 6b),³³ achieving predefined paths of complex trajectories such as “staircase” and
415 “circular” (Fig. 6c).⁴⁰ In addition to the control of individual microrobots, magnetic fields have the
416 capability to manipulate multiple AIMS (Fig. 6d, e)^{44,67} and propel microrobotic swarms too, where
417 individual microrobots assemble into reconfigurable swarming entities that can be actuated and
418 controlled as a whole subject to altering field frequency or strength for enhanced imaging signals
419 *in vivo* (Fig. 6f).³³ Benefiting from the superior actuation and steering performance, MHRs and
420 MTRs have been exploited for on-demand tasks where complex environments are involved. For
421 instance, *SP* MHRs have been controlled to navigate winding microfluidic channels mimicking the
422 gastrointestinal tract.³⁸

423 Although magnetic field control has been widely applied, it also has limitations. Currently, the
424 magnetic fields applied are mostly generated by permanent magnets or electromagnetic coils.
425 Permanent magnets can generate magnetic fields without the use of electric currents, but the field
426 strength decreases rapidly against the distance between the magnet and the working space of
427 microrobots. Furthermore, the direction of the magnetic field can only be altered by physically
428 changing the magnet position, which may not be practical in complicated application scenarios. In
429 contrast to permanent magnets, electromagnetic coils can precisely modulate the magnetic field
430 direction by controlling the input electric currents. However, the temperature of working coils could
431 increase rapidly because of the resistive heating (especially for large coils designed for sufficient
432 working space), thus limiting the operation time and potentially affecting the biological cells inside
433 the workplace too. It should be noted that for rotating magnetic fields, the timing-varying fields
434 might also risk cardiac fibrillation under certain circumstances due to nerve stimulation. This is
435 because the change in the magnetic field gradient can induce electric fields as a function
436 of $d|\mathbf{B}|/dt$, with the maximum rate change [T S⁻¹] for controlled operation described as

$$\frac{d|\mathbf{B}|}{dt} = 20 \left(1 + \frac{0.36}{\tau} \right) \quad (4)$$

438 where τ is the period of the monotonically increasing or decreasing gradient in milliseconds.⁵

440 BIOMEDICAL APPLICATIONS AND BEYOND

441 Micromanipulation

442 AIMS have been extensively applied in micromanipulation tasks, where they function as bio-
443 tweezers, micromotors, micropumps, and micromixers, etc. They were demonstrated to perform
444 tasks with precision such as disrupting biological targets,⁹ pushing submillimeter objects,³⁷
445 manipulating PS microparticles,²⁵ driving synthetic tools,¹⁰⁶ and so on. For example, *CR*-based
446 living micromotors with multiple functions were controlled using OT to destruct biological
447 aggregates, providing a potential tool for localized therapy of blood clots (Fig. 7a).⁹ Shimizu *et al.*
448 innovated a micro pinwheel for trapping four *CR* cells, where the capture components were

449 designed as two rings (diameters 7 μm and 10 μm) to prevent the CR from reversing their directions
450 or escaping. The pinwheel realized rotation via the CR's propulsion force (Fig. 7b).¹⁰⁶ On the other
451 hand, swarming AIMS have been explored to manipulate larger-scale objects (Fig. 7c, d).^{58, 107}
452 Through the phototaxis of AIMS, unidirectional transport of objects can also be achieved with the
453 direction of a light source (Fig. 7e, f).^{22, 37}

454 Apart from using the intact microalgae, their flagella can also be separately exploited for
455 propelling micro-objects. The flagella are easily prepared without complicated purification and
456 reconstitution processes; they tend to attach nonspecifically to surfaces such as a glass tube,¹⁰⁸ and
457 can be reactivated in a controlled manner by adjusting the concentration of ATP in working
458 liquids.¹⁰⁹ Real "artificial flagellates" isolated from CR cells have been attached to the surface of
459 microbeads to make them actuators.³⁰ Biflagellate beads were found capable of moving forward
460 whereas uniflagellate beads only rotated locally, therefore providing general guidelines for
461 designing advanced artificial MFRs.

463 **Active drug delivery**

464 Active delivery of therapeutic cargo or drug payloads through biocompatible AIMS to complex
465 locations or narrow regions inside the human body is promising for precise diagnostics and
466 treatment with minimal side effects. Extensive research was dedicated to this blueprint and some
467 promising proofs of concept have been demonstrated, primarily with microalgae species CR and
468 SP. Several strategies are available for AIMS to load and transport cargo in a controlled manner.
469 CR cells could naturally pick up microscale objects they encounter through electrostatic interaction
470 and carry the cargo forward (Fig. 8a),¹¹⁰ with options to guide the orientation of transportation using
471 a light source.²² Aided by additional magnetic field control, a highly motile biohybrid CR modified
472 by magnetic particles was designed for active cargo delivery and uptake of therapeutics without
473 causing toxic effects (Fig. 8b).³⁴ More recently, algae motors embedded in pH-sensitive degradable
474 capsules were developed for enhanced delivery of drugs to the narrow intestines,⁴³ which achieved
475 prolonged retention within the intestinal mucosa through combining the self-propulsion of CR cells
476 and the protective function of oral capsules (Fig. 8c).

477 SP-based AIMS also play a key role in active cargo delivery. For instance, an MTR featuring
478 porous hollow architecture with high specific surface area (SSA) was designed for effective loading
479 and controlled release of nanoparticles and molecules, e.g., Au NPs and RhB (Fig. 8d).³¹ The natural
480 dehydration and rehydration process of SP cells was found another approach to load molecular
481 cargos (Fig. 8e).³⁸ The delivered molecules can then be released on the target site from the SP cells
482 either through host degradation and/or concentration gradient-driven diffusion, suggesting
483 applications for drug delivery in hard-to-reach regions without invasive operations. Applying this
484 principle, oral delivery of Amifostine for targeted drug accumulation and intestinal protection
485 against cancer radiotherapy was achieved using SP AIMS (Fig. 8f).¹¹¹ Many other works have
486 reported on-demand delivery of therapeutic cargos through AIMS, manifesting the profound
487 potential of AIMS for targeted therapy that would resolve unmet clinical needs.

489 **Anticancer/Antibacterial Therapy**

490 **Anticancer.** In recent years, microalgae have been extensively exploited for enhanced cancer
491 therapy, especially in situations where the therapeutic effects are oxygen-dependent, such as
492 radiotherapy (RT) and photodynamic therapy (PDT). This is because oxygen released by live
493 microalgae cells can potentially alleviate hypoxia in the tumor microenvironment. Furthermore,
494 their intrinsic chlorophyll, an imaging agent for fluorescence (FL) and PA imaging,^{112, 113} could be
495 utilized for reactive oxygen species (ROS) generation upon laser irradiation.^{39, 114} Other bioactive
496 compounds contained by the microalgae cells, such as phycocyanin, were also found capable of
497 selectively killing certain cancer cells.³³ All these desired attributes, taken together, suggest the
498 superiority of microalgae as promising anticancer agents for clinical applications.

499 A series of photosynthetic biosystems engineered from microalgae have been reported to
500 modulate tumor hypoxia through in situ O₂ generation for imaging-guided PDT or RT
501 therapy.^{26,115,116} In these works, *Ch* cells were coated with a protective layer of CaP,¹¹⁵ SiO₂,¹¹⁶ or
502 red blood cell membrane,²⁶ which allowed the microalgae to evade macrophage clearance and reach
503 the tumor sites with maintained photosynthetic activity. To enhance the photodynamic effect, a
504 novel strategy of chlorin e6 (ce6) internalization into *Synechococcus elongatus* has been
505 proposed,¹¹⁷ where O₂ generated by the hybrid microalgae system could be activated into singlet
506 oxygen and satisfactory therapeutic effects on 4T1 tumor cells and xenografts were achieved.

507 The above studies rely on passive accumulation or direct injection of microalgae to the tumor
508 site, without actively steering them. Other efforts have been made to guide AIMs to target the tumor
509 site *in vivo* and mitigate tumor hypoxia to enhance FL/PA/MR imaging-guided therapy (Fig. 9a).³⁹
510 AIMs combined with photothermal therapy (PTT) and chemotherapy have also been developed for
511 targeted delivery and synergistic cancer therapy.²⁷ The Pd@Au core-shell NPs endowed the *SP*
512 microrobots with photothermal effects and the Dox loaded further enabled chemotherapy efficacy
513 (Fig. 9b). Such (Pd@Au)/Fe₃O₄@*SP*-DOX microrobots could be actuated and precisely controlled
514 using magnetic fields and the release of delivered drug could be triggered by pH- and NIR-stimuli.
515 As the temperature rises and the microalgae structure degrades, active biocompounds inside the
516 cells could also be released to selectively kill cancer cells,³³ Furthermore, a swarm of such
517 microrobots could be assembled and disassembled in a controlled manner for targeted Dox delivery,
518 therefore holding promise for navigating narrow regions for anticancer treatment (Fig. 9c).⁴⁴

519 **Antibacterial.** In parallel with anticancer therapy, advanced antibacterial constructs consisting of
520 microalgae and antibacterial materials have been developed to overcome drug resistance and
521 minimize the adverse effects of antibacterial treatment.^{57, 59, 63} This category of AIMs perform
522 antibacterial functions either by releasing loaded antibiotics upon light irradiation or through their
523 photothermal effect endowed by functional coatings. For instance, MFRs for treating infected skin
524 or soft tissue have been facilitated through simplistic chemical surface engineering methods,^{59, 63}
525 where the microalgae cells were modified with antibiotics using a photo-cleavable linker while
526 maintaining their viability, motility, and phototaxis (Fig. 9d). Usually an external light source was
527 applied to guide the direction of the AIM for targeted delivery, followed by release of the
528 antibacterial cargo on-site. Strong inhibition of bacterial growth with high-level spatiotemporal
529 precision has been reported,⁶³ thus verifying the new treatment approach for conventional bacterial
530 infections.
531

532 On the other hand, MHRs consisting of *SP*, Fe₃O₄, and PDA coating were successfully applied
533 for the treatment of multidrug-resistant *Klebsiella pneumoniae* infections in a murine subcutaneous
534 model (Fig. 9e),⁵⁷ where the PDA coating of the microrobots not only enhanced their photothermal
535 effect but also enabled robust PA imaging capability. A swarm of such microrobots could be
536 propelled by a rotating magnetic field with real-time motion tracking under the skin through PA
537 imaging. More recently, microalgae integrated (through click chemistry) with neutrophil
538 membrane-coated polymeric nanoparticles loading antibiotics were designed for acute pneumonia
539 treatment,⁴² which nicely combined the microalgae motility with multifunctional synthetic
540 components. Uniform distribution, low immune clearance, and superb tissue retention time in deep
541 lung tissues were achieved, effectively reducing the bacterial burden. In the future, more generic
542 antibacterial therapy for the treatment of bacterial infections in narrow and complex tissues or
543 cavities should be envisaged. With such therapies, drug resistance and side effects would
544 considerably decrease given the precise treatment in situ for designated time durations.

545 Cell stimulation

546 Cell stimulation is a viable approach for the treatment of nervous system-related diseases, such as
547 Parkinson's disease and myasthenia gravis. The widely applied electrical stimulation has served as
548

549 a feasible strategy, but its application is limited by the inhomogeneity of electric fields and the
550 invasiveness of implanted stimulators.¹¹⁸ Instead, wireless and biocompatible magnetic AIMs hold
551 great promise for precise and efficient neural activation. Recently, Liu *et al.* demonstrated
552 magnetically powered piezoelectric AIMs for precise interactions with neural stem-like cells (Fig.
553 10a).^{45, 66} The tiny AIMs could be accurately guided to a neural stem-like PC12 cell using a rotating
554 magnetic field for the loaded BaTiO₃ NPs to convert ultrasonic energy into electrical signals
555 (through their piezoelectric effect) and induce cell differentiation.⁶⁶ The neuron stem cell activation
556 is accompanied by a sudden calcium ions influx into the cytosol, which depends on the intensity of
557 the electric field and determines the intensity of activation.¹¹⁹ Therefore, directed differentiation of
558 the neural stem cell could be achieved by tuning the intensity of input ultrasound for astrocytes,
559 functional neurons, or oligodendrocytes.⁴⁵ More recently, *Ch*-based AIMs have also been
560 developed to precisely stimulate skeletal muscle contractions with photothermal effect (Fig. 10b).⁴⁶
561 The superparamagnetic microrobots were magnetically navigated to the muscle injury sites and
562 heated upon NIR irradiation, consequently inducing contraction of the muscle fiber through
563 activation of the actin–myosin interactions. In sum, the AIM platforms, wirelessly operated and
564 minimally invasive, provided a promising interventional tool for the treatment of neural system-
565 related or other cellular-level diseases.

566 Other applications

567 In addition to the applications discussed in earlier sections, diverse applications of AIMs are being
568 exploited, *e.g.*, environmental remediation,^{40, 41} on-cell catalysis,³⁶ wound-healing¹²⁰ and
569 biomolecule sensing.²⁸ For instance, an active AIM system consisting of live *CR* cell and an
570 angiotensin-converting enzyme 2 (ACE2) receptor, which is against the SARS-CoV-2 spike
571 proteins (Fig. 10c), has been developed for effective removal of SARS-CoV-2 spike proteins and
572 pseudo-virus from contaminated aquatic media.^{40, 56} Owing to the self-propulsion enabled
573 continuous mixing and collision, the developed AIMs achieved high removal efficacy compared to
574 traditional wastewater treatments, thus offering an efficient tool for pathogenic virus removal and
575 overcoming other threats in contaminated water. *SP*-templated porous hollow AIMs have been
576 explored for the adsorption of heavy metal ions, *e.g.*, Chromium ion (Cr⁶⁺) for water purification
577 (Fig. 10d).⁴¹ Similar to contaminated water, cell culture media may also contain viruses, pathogenic
578 bacteria, or other nano-biothreats. To tackle that, non-invasive methods are required. One such
579 example was diatombot based on *Phaeodactylum tricornutum Bohlin* combining the wake-riding
580 effect and optical trapping, which demonstrated effective trapping and removal of nanoscale bio-
581 targets such as adenoviruses and pathogenic bacteria.¹²¹

582 To enable on-cell catalysis without involving complex transition metal chemistry, artificial
583 metalloenzyme has been grafted on *CR* through surface engineering to provide the cell with
584 versatile chemical capabilities and new reactivity (Fig. 10e).³⁶ The engineered *CR* cells remained
585 viable and could be guided by light in three-dimensional space for potential medical applications.
586 Oxygen-generating *CR* AIMs coated with heparin have been also developed for accelerating wound
587 healing given their ability of in-depth penetration and enhanced retention in the wounded tissue
588 (Fig. 10f), which substantially improved the cytokine scavenging efficiency and alleviated the
589 hypoxic condition associated with diabetic wounds.¹²⁰

590 For low-concentration bioanalysis, existing nanosensors with high sensitivity could detect
591 biological molecules of 1 pM-1 fM,¹²²⁻¹²⁵ but at the price of a long testing window, thus hindering
592 practical application in the clinic. Thanks to the advances in micro-and nanorobotics, the detection
593 speed using biological or synthetic micro/nanomotors can be notably shortened.¹²⁶⁻¹²⁹ However,
594 since the nanoscale sensors could continuously change their position, detecting molecules in real-
595 time or for prolonged duration is difficult, which is commonly required for low-concentration
596 molecule testing. To overcome this issue, *Diatom* frustule-based AIMs have been designed for
597 sensitive, long-time, and position-stable detection of low-concentration DNA molecules in real-
598

599 time (Fig. 10g),²⁸ where the capture speed of molecules was markedly amplified (about four times).
600 The preliminary findings may inspire the rational design of efficient AIMs systems for future
601 sensing of biomarkers.

602 603 **CONCLUSIONS AND OUTLOOK**

604 Thanks to recent advances in nanotechnology and accumulated foundation knowledge across a
605 range of underpinning disciplines (e.g., applied physics, surface chemistry, synthetic biology,
606 materials sciences), AIMs developed for biomedical applications have witnessed remarkable
607 growth in the past decade. Several microrobotic systems have demonstrated bright prospects for
608 clinical translation. A variety of manufacturing methods, bioengineering techniques and
609 actuation/steering strategies have been exploited to enable biomedical applications of AIMs,
610 depicting an unprecedented landscape of revolutionizing future healthcare with precision medicine
611 strategies such as active drug delivery and targeted therapy. Notwithstanding the fact that multiple
612 AIMs have been assessed with experimental models and evaluated in rodents as well as larger
613 animals, crucial challenges remain to be addressed for steady translation of these microrobots into
614 practical therapies in clinics for benefiting patients. To enlighten solutions for bridging the gap, we
615 provide our perspectives on the current challenges and future directions of AIM research as below.

616 617 **Current challenges**

618 With substantial technological breakthroughs and diversifying target applications, AIMs have come
619 to a crossroad of challenges and opportunities. Although the volume of AIM research keeps
620 expanding, critical hurdles persist and need to be satisfactorily overcome before bench-to-bed
621 translation is possible. These hurdles include but are not limited to, cost-effectiveness of mass
622 production, safety hazards of human administration, inconsistent precision of untethered control,
623 insufficient accuracy of remote tracking, unclear pathway of *in vivo* degradation/retrieval and
624 undesired ambiguity of long-term toxicity. The focus of much AIM research remains on exploratory
625 developments in petri dish or incremental understanding of AIM's biophysical/biochemical
626 behavior, rather than enhancing the technological basis of reported studies or advancing their
627 clinical assessment for progressive translation. Whereas such a focus may contribute to novel
628 concepts and more publications in the near future, they may hinder the substantiation and
629 advancements of promising AIMs that have gone through systematic assessment *in vitro*, *ex vivo*
630 or *in vivo*. Furthermore, there is a lack of international standard or unanimous criteria for
631 consistently evaluating and reporting the clinical relevance and potential ethical implications of
632 studied AIMs when certain biomedical applications are claimed or envisioned. The challenges
633 stated above shed light on valuable opportunities and future directions of AIM research that could
634 stimulate the field in significant measures through concerted research efforts, which we present
635 next.

636 637 **Future directions**

638 There are several key directions of research that can help accelerate the translation of AIMs toward
639 realistic biomedical applications in clinics.

640 **Fabrication.** Consolidation and/or innovation of cost-effective methods for manufacturing AIMs
641 out of currently used or newly developed microalgae, which is essential to sustainable fabrication
642 of AIMs with designated maneuverability and functionalities suiting dynamical conditions one
643 would expect in the human body. On the one hand, abundant candidates of microalgae in nature
644 remain to be discovered or mimicked for developing versatile AIMs to meet more demanding
645 scenarios which reflect the multifold uncertainty in a physiological environment, e.g., cellular
646 interactions, biological barriers and immune responses. On the other hand, core functions of
647 existing AIMs (e.g., biocompatibility, degradability, therapeutic activity) should be sufficiently
648 multiplexed through integration of intrinsic microalgae attributes and smart surface engineering.

649 **Navigation.** Automated redesign and iterative refinement of AIMs with the aid of artificial
650 intelligence and bio-inspired engineering, preferably incorporating embodied intelligence of
651 microorganisms in nature, which will help advance mature AIMs (e.g., those already evaluated with
652 animal models *in vivo*) toward scalable production and potential commercialization. From a
653 technological perspective, the actuation system and steering methods of AIMs should be rigorously
654 evaluated for well-defined application scenes, primarily meeting three requirements: (i) responsive
655 and intelligent feedback adapting to operator instructions; (ii) robust and precise locomotion
656 accommodating hard-to-reach environments; (iii) reliable and spontaneous imaging equipped for
657 close-loop control.

658
659 **Translation.** Co-design and co-delivery of meaningful AIM proofs of concept with clinicians from
660 early stage to align research with clinical needs and streamline a path to practical therapies or
661 medical treatments. The top-down approach will likely lead to engaging projects and impactful
662 outcomes with clear socioeconomic benefits for facilitating organizational support, industrial
663 engagement and regulatory approval. Such projects require interdisciplinary collaboration and
664 knowledge exchange among researchers from diverse backgrounds (e.g., materials scientists,
665 nanoengineers, chemists, roboticist) and clinical practitioners in the frontline (e.g., physicians,
666 surgeons). One emerging trend in the research field of AIMs is that researchers with less relevant
667 backgrounds (e.g., fluid dynamists, computational modelers) are also growingly involved, who may
668 contribute to fundamental understanding and optimization pathway of AIMs in complex biofluids
669 and physiological environments through mechanistic models and digital twins.

670 **Concluding remarks**

671
672 To sum up, AIMs are still in their infancy but with transformative promises in shaping precision
673 medicine and stratified healthcare. We hope this article has provided a useful overview of recent
674 progresses on the design and application of algae-inspired microrobots as well as their underlying
675 biological and technological foundations, in the anticipation of fostering greater technological
676 innovation and deeper pre-clinical developments as the stepping stones for clinical translation.

677 **References**

- 678 1. W. Gao, A. Uygun, J. Wang, Hydrogen-bubble-propelled Zinc-based microrockets in strongly acidic
679 media. *J. Am. Chem. Soc.* **134**, 897-900 (2012).
- 680 2. L. Liu, M. Liu, Y. Su, Y. Dong, W. Zhou, L. Zhang, H. Zhang, B. Dong, L. Chi, Tadpole-like artificial
681 micromotor. *Nanoscale* **7**, 2276-2280 (2015).
- 682 3. R. Liu, A. Sen, Autonomous nanomotor based on copper-platinum segmented nanobattery. *J. Am. Chem.*
683 *Soc.* **133**, 20064-20067 (2011).
- 684 4. J. Wang, W. Gao, Nano/microscale motors: biomedical opportunities and challenges. *ACS Nano* **6**, 5745-
685 5751 (2012).
- 686 5. B. J. Nelson, I. K. Kaliakatsos, J. J. Abbott, Microrobots for minimally invasive medicine. *Annu. Rev.*
687 *Biomed. Eng.* **12**, 55-85 (2010).
- 688 6. M. Sitti, H. Ceylan, W. Hu, J. Giltinan, M. Turan, S. Yim, E. Diller, Biomedical applications of untethered
689 mobile milli/microrobots. *Proc. IEEE* **103**, 205-224 (2015).
- 690 7. J. Li, B. Esteban-Fernandez de Avila, W. Gao, L. Zhang, J. Wang, Micro/nanorobots for biomedicine:
691 delivery, surgery, sensing, and detoxification. *Sci. Robot.* **2**, eaam6431 (2017).
- 692 8. J. Katuri, X. Ma, M. M. Stanton, S. Sanchez, Designing micro- and nanoswimmers for specific
693 applications. *Acc. Chem. Res.* **50**, 2-11 (2017).
- 694 9. H. Xin, N. Zhao, Y. Wang, X. Zhao, T. Pan, Y. Shi, B. Li, Optically controlled living micromotors for the
695 manipulation and disruption of biological targets. *Nano Lett.* **20**, 7177-7185 (2020).
- 696 10. J. Christensen, L. Norgaard, R. Bro, S. B. Engelsen, Multivariate autofluorescence of intact food systems.
697 *Chem. Rev.* **106**, 1979-1994 (2006).
- 698 11. T.-X. Fan, S.-K. Chow, D. Zhang, Biomorphic mineralization: from biology to materials. *Prog. Mater.*
699 *Sci.* **54**, 542-659 (2009).
- 700 12. B. Metting, J. W. Pyne, Biologically-active compounds from microalgae. *Enzyme Microb. Technol.* **8**,
- 701

- 386-394 (1986).
- 703 13. A. R. Parker, H. E. Townley, Biomimetics of photonic nanostructures. *Nat. Nanotechnol.* **2**, 347-353
704 (2007).
 - 705 14. P.-Y. Chen, J. McKittrick, M. A. Meyers, Biological materials: functional adaptations and bioinspired
706 designs. *Prog. Mater. Sci.* **57**, 1492-1704 (2012).
 - 707 15. N. Billinton, A. W. Knight, Seeing the wood through the trees: a review of techniques for distinguishing
708 green fluorescent protein from endogenous autofluorescence. *Anal. Biochem.* **291**, 175-197 (2001).
 - 709 16. S. Martel, M. Mohammadi, O. Felfoul, Z. Lu, P. Pouponneau, Flagellated magnetotactic bacteria as
710 controlled MRI-trackable propulsion and steering systems for medical nanorobots operating in the human
711 microvasculature. *Int. J. Robot. Res.* **28**, 571-582 (2009).
 - 712 17. V. Magdanz, S. Sanchez, O. G. Schmidt, Development of a sperm-flagella driven micro-bio-robot. *Adv.*
713 *Mater.* **25**, 6581-6588 (2013).
 - 714 18. R. W. Carlsen, M. Sitti, Bio-hybrid cell-based actuators for microsystems. *Small* **10**, 3831-3851 (2014).
 - 715 19. C. Sanchez, H. Arribart, M. M. G. Guille, Biomimetism and bioinspiration as tools for the design of
716 innovative materials and systems. *Nat. Mater.* **4**, 277-288 (2005).
 - 717 20. H. Wang, M. Pumera, Fabrication of micro/nanoscale motors. *Chem. Rev.* **115**, 8704-8735 (2015).
 - 718 21. M. B. Akolpoglu, N. O. Dogan, U. Bozuyuk, H. Ceylan, S. Kizilel, M. Sitti, High-yield production of
719 biohybrid microalgae for on-demand cargo delivery. *Adv. Sci.* **7**, 2001256 (2020).
 - 720 22. D. B. Weibel, P. Garstecki, D. Ryan, W. R. DiLuzio, M. Mayer, J. E. Seto, G. M. Whitesides, Microoxen:
721 microorganisms to move microscale loads. *Proc. Natl. Acad. Sci. U. S. A.* **102**, 11963-11967 (2005).
 - 722 23. J. Wang, F. Soto, S. Q. Liu, Q. Q. Yin, E. Purcell, Y. T. Zeng, E. C. Hsu, D. Akin, B. Sinclair, T. Stoyanova,
723 U. Demirci, Volbots: Volvox microalgae-based robots for multimode precision imaging and therapy. *Adv.*
724 *Funct. Mater.* **32**, 2201800 (2022).
 - 725 24. S. Xie, N. Jiao, S. Tung, L. Liu, Controlled regular locomotion of algae cell microrobots. *Biomed.*
726 *Microdevices* **18**, 47 (2016).
 - 727 25. C. Zhang, S. X. Xie, W. X. Wang, N. Xi, Y. C. Wang, L. Q. Liu, Bio-syncretic tweezers actuated by
728 microorganisms: modeling and analysis. *Soft Matter* **12**, 7485-7494 (2016).
 - 729 26. Y. Qiao, F. Yang, T. Xie, Z. Du, D. Zhong, Y. Qi, Y. Li, W. Li, Z. Lu, J. Rao, Y. Sun, M. Zhou, Engineered
730 algae: a novel oxygen-generating system for effective treatment of hypoxic cancer. *Sci. Adv.* **6**, eaba5996
731 (2020).
 - 732 27. X. Wang, J. Cai, L. Sun, S. Zhang, D. Gong, X. Li, S. Yue, L. Feng, D. Zhang, Facile fabrication of
733 magnetic microrobots based on *Spirulina* templates for targeted delivery and synergistic chemo-
734 photothermal therapy. *ACS Appl. Mater. Interfaces* **11**, 4745-4756 (2019).
 - 735 28. J. Guo, Z. Liang, Y. Huang, K. Kim, P. Vandeventer, D. Fan, Acceleration of biomolecule enrichment
736 and detection with rotationally motorized opto-plasmonic microsensors and the working mechanism.
737 *ACS Nano* **14**, 15204-15215 (2020).
 - 738 29. C. Yao, J. Jiang, X. Cao, Y. Liu, S. Xue, Y. Zhang, Phosphorus enhances photosynthetic storage starch
739 production in a green microalga (chlorophyta) *Tetraselmis subcordiformis* in nitrogen starvation
740 conditions. *J. Agric. Food Chem.* **66**, 10777-10787 (2018).
 - 741 30. N. Mori, K. Kuribayashi, S. Takeuchi, Artificial flagellates: analysis of advancing motions of biflagellate
742 micro-objects. *Appl. Phys. Lett.* **96**, 083701 (2010).
 - 743 31. X. Yan, Q. Zhou, J. F. Yu, T. T. Xu, Y. Deng, T. Tang, Q. Feng, L. M. Bian, Y. Zhang, A. Ferreira, L.
744 Zhang, Magnetite nanostructured porous hollow helical microswimmers for targeted delivery. *Adv. Funct.*
745 *Mater.* **25**, 5333-5342 (2015).
 - 746 32. T. Hatsuzawa, D. Ito, T. Nisisako, Y. Yanagida, Micro-rotary ratchets driven by migratory phytoplankton
747 with phototactic stimulus. *Precis. Eng.* **48**, 107-113 (2017).
 - 748 33. X. Yan, Q. Zhou, M. Vincent, Y. Deng, J. Yu, J. Xu, T. Xu, T. Tang, L. Bian, Y. J. Wang, K. Kostarelos,
749 L. Zhang, Multifunctional biohybrid magnetite microrobots for imaging-guided therapy. *Sci. Robot.* **2**,
750 eaaq1155 (2017).
 - 751 34. O. Yasa, P. Erkoç, Y. Alapan, M. Sitti, Microalga-powered microswimmers toward active cargo delivery.
752 *Adv. Mater.* **30**, e1804130 (2018).
 - 753 35. D. Gong, J. Cai, N. Celi, L. Feng, Y. G. Jiang, D. Zhang, Bio-inspired magnetic helical microswimmers
754 made of nickel-plated *Spirulina* with enhanced propulsion velocity. *J. Magn. Magn. Mater.* **468**, 148-154
755 (2018).
 - 756 36. M. Szponarski, F. Schwizer, T. R. Ward, K. Gademann, On-cell catalysis by surface engineering of live
757 cells with an artificial metalloenzyme. *Commun. Chem.* **1**, 84 (2018).
 - 758 37. M. Nagai, T. Hirano, T. Shibata, Phototactic algae-driven unidirectional transport of submillimeter-sized
759 cargo in a microchannel. *Micromachines* **10**, 130 (2019).

- 760 38. X. H. Yan, J. B. Xu, Q. Zhou, D. D. Jin, C. A. Vong, Q. Feng, D. H. L. Ng, L. Bian, L. Zhang, Molecular
761 cargo delivery using multicellular magnetic microswimmers. *Appl. Mater. Today* **15**, 242-251 (2019).
- 762 39. D. N. Zhong, W. L. Li, Y. C. Qi, J. He, M. Zhou, Photosynthetic biohybrid nanoswimmers system to
763 alleviate tumor hypoxia for FL/PA/MR imaging-guided enhanced radio-photodynamic synergetic therapy.
764 *Adv. Funct. Mater.* **30**, 1910395 (2020).
- 765 40. F. Zhang, Z. Li, L. Yin, Q. Zhang, N. Askarinam, R. Mundaca-Uribe, F. Tehrani, E. Karshalev, W. Gao,
766 L. Zhang, J. Wang, ACE2 receptor-modified algae-based microrobot for removal of SARS-CoV-2 in
767 wastewater. *J. Am. Chem. Soc.* **143**, 12194-12201 (2021).
- 768 41. C. Zheng, Z. Li, T. Xu, L. Chen, F. Fang, D. Wang, P. Dai, Q. Wang, X. Wu, X. Yan, *Spirulina*-templated
769 porous hollow carbon@magnetite core-shell microswimmers. *Appl. Mater. Today* **22**, 100962 (2021).
- 770 42. F. Zhang, J. Zhuang, Z. Li, H. Gong, B. E. de Avila, Y. Duan, Q. Zhang, J. Zhou, L. Yin, E. Karshalev,
771 W. Gao, V. Nizet, R. Fang, L. Zhang, J. Wang, Nanoparticle-modified microrobots for *in vivo* antibiotic
772 delivery to treat acute bacterial pneumonia. *Nat. Mater.* **21**, 1324-1332 (2022).
- 773 43. F. Zhang, Z. Li, Y. Duan, A. Abbas, R. Mundaca-Uribe, L. Yin, H. Luan, W. Gao, R. H. Fang, L. Zhang,
774 J. Wang, Gastrointestinal tract drug delivery using algae motors embedded in a degradable capsule. *Sci.*
775 *Robot.* **7**, eabo4160 (2022).
- 776 44. D. Gong, N. Celi, D. Zhang, J. Cai, Magnetic biohybrid microrobot multimers based on *Chlorella* cells
777 for enhanced targeted drug delivery. *ACS Appl. Mater. Interfaces* **14**, 6320-6330 (2022).
- 778 45. L. Liu, J. Wu, S. Wang, K. Liu, J. B. Gao, B. Chen, Y. C. Ye, F. Wang, F. Tong, J. M. Jiang, J. F. Ou, D.
779 A. Wilson, Y. F. Tu, F. Peng, Control the neural stem cell fate with biohybrid piezoelectrical magnetite
780 micromotors. *Nano Lett.* **21**, 9361-9363 (2021).
- 781 46. L. Liu, J. Wu, B. Chen, J. Gao, T. Li, Y. Ye, H. Tian, S. Wang, F. Wang, J. Jiang, J. Ou, F. Tong, F. Peng,
782 Y. Tu, Magnetically actuated biohybrid microswimmers for precise photothermal muscle contraction.
783 *ACS Nano* **16**, 6515-6526 (2022).
- 784 47. S. Liu, H. Yang, M. Y. Ho, B. Xing, Recent advances of material-decorated photosynthetic
785 microorganisms and their aspects in biomedical applications. *Adv. Opt. Mater.* **11**, 2203038 (2023).
- 786 48. D. Gong, L. Sun, X. Li, W. Zhang, D. Zhang, J. Cai, Micro/nanofabrication, assembly, and actuation
787 based on microorganisms: recent advances and perspectives. *Small Struct.* **4**, 2200356 (2023).
- 788 49. D. Zhong, Z. Du, M. Zhou, Algae: a natural active material for biomedical applications. *View* **2**, 20200189
789 (2021).
- 790 50. Z. Zhang, Y. Chen, L. H. Klausen, S. A. Skaanvik, D. Wang, J. Chen, M. Dong, The rational design and
791 development of microalgae-based biohybrid materials for biomedical applications. *Engineering* **24**, 102-
792 113 (2023).
- 793 51. D. Quashie, Jr., P. Benhal, Z. Chen, Z. Wang, X. Mu, X. Song, T. Jiang, Y. Zhong, U. K. Cheang, J. Ali,
794 Magnetic bio-hybrid micro actuators. *Nanoscale* **14**, 4364-4379 (2022).
- 795 52. W. Wang, W. T. Duan, S. Ahmed, T. E. Mallouk, A. Sen, Small power: autonomous nano- and
796 micromotors propelled by self-generated gradients. *Nano Today* **8**, 531-554 (2013).
- 797 53. E. H. Harris, *Chlamydomonas* as a model organism. *Annu. Rev. Plant Physiol. Plant Mol. Biol.* **52**, 363-
798 406 (2001).
- 799 54. R. Hirschberg, S. Rodgers, Chemoresponses of *Chlamydomonas reinhardtii*. *J. Bacteriol.* **134**, 671-673
800 (1978).
- 801 55. Y. Hayashi, K. Sugawara, Simultaneous coupling of phototaxis and electrotaxis in *Volvox algae*. *Phys.*
802 *Rev. E* **89**, 042714 (2014).
- 803 56. J. L. Lai, Q. F. Meng, M. Y. Tian, X. Y. Zhuang, P. Pan, L. A. Du, L. Deng, J. Y. Tang, N. Y. Jin, L. Rao,
804 A decoy microrobot that removes SARS-CoV-2 and its variants in wastewater. *Cell Rep. Phys. Sci.* **3**,
805 101061 (2022).
- 806 57. L. Xie, X. Pang, X. Yan, Q. Dai, H. Lin, J. Ye, Y. Cheng, Q. Zhao, X. Ma, X. Zhang, G. Liu, X. Chen,
807 Photoacoustic imaging-trackable magnetic microswimmers for pathogenic bacterial infection treatment.
808 *ACS Nano* **14**, 2880-2893 (2020).
- 809 58. S. X. Xie, L. L. Qin, G. X. Li, N. A. D. Jiao, Robotized algal cells and their multiple functions. *Soft*
810 *Matter* **17**, 3047-3054 (2021).
- 811 59. I. P. Kerschgens, K. Gademann, Antibiotic algae by chemical surface engineering. *ChemBiochem* **19**,
812 439-443 (2018).
- 813 60. G. Santomauro, A. V. Singh, B. W. Park, M. Mohammadrahimi, P. Erkoç, E. Goering, G. Schütz, M. Sitti,
814 J. Bill, Incorporation of Terbium into a microalga leads to magnetotactic swimmers. *Adv. Biosyst.* **2**,
815 1800039 (2018).
- 816 61. W. M. Ng, H. X. Che, C. Guo, C. Liu, S. C. Low, D. J. Chieh Chan, R. Mohamud, J. Lim, Artificial
817 magnetotaxis of microbot: magnetophoresis versus self-swimming. *Langmuir* **34**, 7971-7980 (2018).

- 818 62. I. S. Shchelik, J. V. D. Molino, K. Gademann, Biohybrid microswimmers against bacterial infections. *Acta Biomater.* **136**, 99-110 (2021).
- 819
- 820 63. I. S. Shchelik, S. Sieber, K. Gademann, Green algae as a drug delivery system for the controlled release
821 of antibiotics. *Chem. Eur. J.* **26**, 16644-16648 (2020).
- 822 64. D. Gong, J. Cai, N. Celi, C. Liu, W. Q. Zhang, L. Feng, D. Y. Zhang, Controlled propulsion of wheel-
823 shape flaky microswimmers under rotating magnetic fields. *Appl. Phys. Lett.* **114**, 123701 (2019).
- 824 65. D. Gong, N. Celi, L. Xu, D. Zhang, J. Cai, CuS nanodots-loaded biohybrid magnetic helical microrobots
825 with enhanced photothermal performance. *Mater. Today Chem.* **23**, 100694 (2022).
- 826 66. L. Liu, B. Chen, K. Liu, J. Gao, Y. Ye, Z. Wang, N. Qin, D. A. Wilson, Y. Tu, F. Peng, Wireless
827 manipulation of magnetic/piezoelectric micromotors for precise neural stem-like cell stimulation. *Adv.*
828 *Funct. Mater.* **30**, 1910108 (2020).
- 829 67. M. Li, J. Wu, D. Lin, J. Yang, N. Jiao, Y. Wang, L. Liu, A diatom-based biohybrid microrobot with a high
830 drug-loading capacity and pH-sensitive drug release for target therapy. *Acta Biomater.* **154**, 443-453
831 (2022).
- 832 68. E. Lauga, T. R. Powers, The hydrodynamics of swimming microorganisms. *Rep. Prog. Phys.* **72**, 096601
833 (2009).
- 834 69. B. Behkam, M. Sitti, Design methodology for biomimetic propulsion of miniature swimming robots. *J.*
835 *Dyn. Syst-T. Asme.* **128**, 36-43 (2006).
- 836 70. X. Garcia, S. Rafai, P. Peyla, Light control of the flow of phototactic microswimmer suspensions. *Phys.*
837 *Rev. Lett.* **110**, 138106 (2013).
- 838 71. G. J. Pazour, N. Agrin, J. Leszyk, G. B. Witman, Proteomic analysis of a eukaryotic cilium. *J. Cell Biol.*
839 **170**, 103-113 (2005).
- 840 72. C. Shingyoji, H. Higuchi, M. Yoshimura, E. Katayama, T. Yanagida, Dynein arms are oscillating force
841 generators. *Nature* **393**, 711-714 (1998).
- 842 73. C. J. Brokaw, R. Kamiya, Bending patterns of *Chlamydomonas* flagella: IV. Mutants with defects in inner
843 and outer dynein arms indicate differences in dynein arm function. *Cell Motil. Cytoskeleton* **8**, 68-75
844 (1987).
- 845 74. R. Ahmad, C. Kleineberg, V. Nasirimarekani, Y. J. Su, S. G. Pozveh, A. Bae, K. Sundmacher, E.
846 Bodenschatz, I. Guido, T. Vidakovic-Koch, A. Gholami, Light-powered reactivation of flagella and
847 contraction of microtubule networks: toward building an artificial cell. *ACS Synth. Biol.* **10**, 1490-1504
848 (2021).
- 849 75. E. F. Smith, W. S. Sale, Regulation of dynein-driven microtubule sliding by the radial spokes in flagella.
850 *Science* **257**, 1557-1559 (1992).
- 851 76. D. Luck, G. Piperno, Z. Ramanis, B. Huang, Flagellar mutants of *Chlamydomonas*: studies of radial
852 spoke-defective strains by dikaryon and revertant analysis. *Proc. Natl. Acad. Sci. U. S. A.* **74**, 3456-3460
853 (1977).
- 854 77. N. Ueki, T. Ide, S. Mochiji, Y. Kobayashi, R. Tokutsu, N. Ohnishi, K. Yamaguchi, S. Shigenobu, K.
855 Tanaka, J. Minagawa, T. Hisabori, M. Hirono, K. Wakabayashi, Eyespot-dependent determination of the
856 phototactic sign in *Chlamydomonas reinhardtii*. *Proc. Natl. Acad. Sci. U. S. A.* **113**, 5299-5304 (2016).
- 857 78. R. R. Bennett, R. Golestanian, A steering mechanism for phototaxis in *Chlamydomonas*. *J. R. Soc.*
858 *Interface* **12**, 20141164 (2015).
- 859 79. O. Tainio, F. Sohrabi, N. Janarek, J. Koivisto, A. Puisto, L. Viitanen, J. V. I. Timonen, M. Alava,
860 *Chlamydomonas reinhardtii* swimming in the Plateau borders of 2D foams. *Soft Matter* **17**, 145-152
861 (2021).
- 862 80. U. Ruffer, W. Nultsch, High-speed cinematographic analysis of the movement of *Chlamydomonas*. *Cell*
863 *Motil. Cytoskeleton* **5**, 251-263 (1985).
- 864 81. H. Harz, C. Nonnengasser, P. Hegemann, The photoreceptor current of the green alga *Chlamydomonas*.
865 *Philos. T. R. Soc. B.* **338**, 39-52 (1992).
- 866 82. K. Schaller, R. David, R. Uhl, How *Chlamydomonas* keeps track of the light once it has reached the right
867 phototactic orientation. *Biophys. J.* **73**, 1562-1572 (1997).
- 868 83. H. Harz, P. Hegemann, Rhodopsin-regulated calcium currents in *Chlamydomonas*. *Nature* **351**, 489-491
869 (1991).
- 870 84. E. M. Holland, F. J. Braun, C. Nonnengasser, H. Harz, P. Hegemann, The nature of rhodopsin-triggered
871 photocurrents in *Chlamydomonas*. I. Kinetics and influence of divalent ions. *Biophys. J.* **70**, 924-931
872 (1996).
- 873 85. K. W. Foster, R. D. Smyth, Light antennas in phototactic algae. *Microbiol. Rev.* **44**, 572-630 (1980).
- 874 86. D. G. Grier, A revolution in optical manipulation. *Nature* **424**, 810-816 (2003).
- 875 87. H. Xin, Y. Li, D. Xu, Y. Zhang, C. Chen, B. Li, Single upconversion nanoparticle-bacterium cotrapping

- 876 for single-bacterium labeling and analysis. *Small* **13**, 1603418 (2017).
- 877 88. K. Norregaard, R. Metzler, C. M. Ritter, K. Berg-Sorensen, L. B. Oddershede, Manipulation and motion
878 of organelles and single molecules in living cells. *Chem. Rev.* **117**, 4342-4375 (2017).
- 879 89. J. L. Killian, F. Ye, M. D. Wang, Optical tweezers: a force to be reckoned with. *Cell* **175**, 1445-1448
880 (2018).
- 881 90. H. B. Xin, Y. C. Li, Y. C. Liu, Y. Zhang, Y. F. Xiao, B. J. Li, Optical forces: from fundamental to biological
882 applications. *Adv. Mater.* **32**, 2001994 (2020).
- 883 91. R. P. Sinha, D. P. Häder, UV-induced DNA damage and repair: a review. *Photochem. Photobiol. Sci.* **1**,
884 225-236 (2002).
- 885 92. D. I. Pattison, M. J. Davies, Actions of ultraviolet light on cellular structures. In *Cancer: Cell Structures,*
886 *Carcinogens and Genomic Instability*, Experientia Supplementum, vol 96, pp 131-157. Birkhäuser Basel:
887 Basel, 2006.
- 888 93. R. S. M. Rikken, R. J. M. Nolte, J. C. Maan, J. C. M. van Hest, D. A. Wilson, P. C. M. Christianen,
889 Manipulation of micro- and nanostructure motion with magnetic fields. *Soft Matter* **10**, 1295-1308 (2014).
- 890 94. S. Martel, Beyond imaging: Macro- and microscale medical robots actuated by clinical MRI scanners.
891 *Sci. Robot.* **2**, eaam8119 (2017).
- 892 95. J. Zhuang, M. Sitti, Chemotaxis of bio-hybrid multiple bacteria-driven microswimmers. *Sci. Rep.* **6**,
893 32135 (2016).
- 894 96. D. Kim, A. Liu, E. Diller, M. Sitti, Chemotactic steering of bacteria propelled microbeads. *Biomed.*
895 *Microdevices* **14**, 1009-1017 (2012).
- 896 97. B. Cortese, I. E. Palamà, S. D'Amone, G. Gigli, Influence of electrotaxis on cell behavior. *Integr. Biol.* **6**,
897 817-830 (2014).
- 898 98. T. Y. Tsong, Electroporation of cell-membranes. *Biophys. J.* **60**, 297-306 (1991).
- 899 99. T. H. Tran, D. H. Kim, J. Kim, M. J. Kim, D. Byun, Use of an AC electric field in galvanotactic on/off
900 switching of the motion of a microstructure blotted by *Serratia marcescens*. *Appl. Phys. Lett.* **99**, 063702
901 (2011).
- 902 100. S. Tottori, L. Zhang, F. M. Qiu, K. K. Krawczyk, A. Franco-Obregón, B. J. Nelson, Magnetic helical
903 micromachines: fabrication, controlled swimming, and cargo transport. *Adv. Mater.* **24**, 811-816 (2012).
- 904 101. W. Wang, L. A. Castro, M. Hoyos, T. E. Mallouk, Autonomous motion of metallic microrods propelled
905 by ultrasound. *ACS Nano* **6**, 6122-6132 (2012).
- 906 102. S. Palagi, A. G. Mark, S. Y. Reigh, K. Melde, T. Qiu, H. Zeng, C. Parmeggiani, D. Martella, A. Sanchez-
907 Castillo, N. Kapernaum, F. Giesselmann, D. S. Wiersma, E. Lauga, P. Fischer, Structured light enables
908 biomimetic swimming and versatile locomotion of photoresponsive soft microrobots. *Nat. Mater.* **15**,
909 647-653 (2016).
- 910 103. J. J. Abbott, K. E. Peyer, M. C. Lagomarsino, L. Zhang, L. X. Dong, I. K. Kaliakatsos, B. J. Nelson, How
911 should microrobots swim? *Int. J. Robot. Res.* **28**, 1434-1447 (2009).
- 912 104. K. Bente, A. Codutti, F. Bachmann, D. Faivre, Biohybrid and bioinspired magnetic microswimmers.
913 *Small* **14**, 1704374 (2018).
- 914 105. K. I. Morozov, Y. Mirzae, O. Kenneth, A. M. Leshansky, Dynamics of arbitrary shaped propellers driven
915 by a rotating magnetic field. *Phys. Rev. Fluids* **2**, 044202 (2017).
- 916 106. N. Shimizu, H. Oda, Y. Morimoto, S. Takeuchi, Biohybrid micro pinwheel powered by trapped
917 microalgae. *2021 IEEE 34th International Conference on Micro Electro Mechanical Systems (MEMS),*
918 *Gainesville, FL, USA, 2021*, pp. 533-535. doi: 10.1109/MEMS51782.2021.9375193.
- 919 107. X. D. Wang, N. D. Jiao, S. Tung, L. Q. Liu, Locomotion of microstructures driven by algae cells. *2018*
920 *International Conference on Manipulation, Automation and Robotics at Small Scales (MARSS), Nagoya,*
921 *Japan, 2018*, pp. 1-5. doi: 10.1109/MARSS.2018.8481168.
- 922 108. R. Kamiya, G. B. Witman, Submicromolar levels of calcium control the balance of beating between the
923 two flagella in demembrated models of *Chlamydomonas*. *J. Cell Biol.* **98**, 97-107 (1984).
- 924 109. R. Yokokawa, S. Takeuchi, T. Kon, M. Nishiura, R. Ohkura, K. Sutoh, H. Fujita, Hybrid nanotransport
925 system by biomolecular linear motors. *J. Microelectromech. Syst.* **13**, 612-619 (2004).
- 926 110. X. J. Teng, W. M. Ng, W. H. Chong, D. J. C. Chan, R. Mohamud, B. S. Ooi, C. Guo, C. Z. Liu, J. Lim,
927 The transport behavior of a biflagellated microswimmer before and after cargo loading. *Langmuir* **37**,
928 9192-9201 (2021).
- 929 111. D. X. Zhang, D. N. Zhong, J. Ouyang, J. He, Y. C. Qi, W. Chen, X. C. Zhang, W. Tao, M. Zhou,
930 Microalgae-based oral microcarriers for gut microbiota homeostasis and intestinal protection in cancer
931 radiotherapy. *Nat. Commun.* **13**, 1413 (2022).
- 932 112. R. K. Pandey, L. N. Goswami, Y. H. Chen, A. Gryshuk, J. R. Missert, A. Oseroff, T. J. Dougherty, Nature:
933 A rich source for developing multifunctional agents. tumor-imaging and photodynamic therapy. *Lasers*

- 934 *Surg. Med.* **38**, 445-467 (2006).
- 935 113. E. H. Murchie, T. Lawson, Chlorophyll fluorescence analysis: a guide to good practice and understanding
936 some new applications. *J. Exp. Bot.* **64**, 3983-3998 (2013).
- 937 114. V. Rizzi, P. Fini, F. Fanelli, T. Placido, P. Semeraro, T. Sibillano, A. Fraix, S. Sortino, A. Agostiano, C.
938 Giannini, P. Cosma, Molecular interactions, characterization and photoactivity of Chlorophyll
939 a/chitosan/2-HP- β -cyclodextrin composite films as functional and active surfaces for ROS production.
940 *Food Hydrocolloids* **58**, 98-112 (2016).
- 941 115. D. N. Zhong, W. L. Li, S. Y. Hua, Y. C. Qi, T. T. Xie, Y. Qiao, M. Zhou, Calcium phosphate engineered
942 photosynthetic microalgae to combat hypoxic-tumor by in-situ modulating hypoxia and cascade radio-
943 phototherapy. *Theranostics* **11**, 3580-3594 (2021).
- 944 116. W. L. Li, D. N. Zhong, S. Y. Hua, Z. Du, M. Zhou, Biom mineralized biohybrid algae for tumor hypoxia
945 modulation and cascade radio-photodynamic therapy. *ACS Appl. Mater. Interfaces* **12**, 44541-44553
946 (2020).
- 947 117. M. F. Huo, L. Y. Wang, L. L. Zhang, C. Y. Wei, Y. Chen, J. L. Shi, Photosynthetic tumor oxygenation by
948 photosensitizer-containing cyanobacteria for enhanced photodynamic therapy. *Angew. Chem.* **59**, 1906-
949 1913 (2020).
- 950 118. R. Zhu, Z. Q. Sun, C. P. Li, S. Ramakrishna, K. Chiu, L. M. He, Electrical stimulation affects neural stem
951 cell fate and function in vitro. *Exp. Neurol.* **319**, 112963 (2019).
- 952 119. M. D'Ascenzo, R. Piacentini, P. Casalbore, M. Budoni, R. Pallini, G. B. Azzena, C. Grassi, Role of L-
953 type Ca²⁺ channels in neural stem/progenitor cell differentiation. *Eur. J. Neurosci.* **23**, 935-944 (2006).
- 954 120. H. Choi, B. Kim, S. H. Jeong, T. Y. Kim, D. P. Kim, Y. K. Oh, S. K. Hahn, Microalgae-based biohybrid
955 microrobot for accelerated diabetic wound healing. *Small* **19**, e2204617 (2023).
- 956 121. J. Xiong, Y. Shi, T. Pan, D. Lu, Z. He, D. Wang, X. Li, G. Zhu, B. Li, H. Xin, Wake-riding effect-inspired
957 opto-hydrodynamic Diatombot for non-invasive trapping and removal of nano-biothreats. *Adv. Sci.* **10**,
958 e2301365 (2023).
- 959 122. Y. Weizmann, F. Patolsky, I. Willner, Amplified detection of DNA and analysis of single-base mismatches
960 by the catalyzed deposition of gold on Au-nanoparticles. *Analyst* **126**, 1502-1504 (2001).
- 961 123. E. D. Goluch, J. M. Nam, D. G. Georganopoulou, T. N. Chiesl, K. A. Shaikh, K. S. Ryu, A. E. Barron, C.
962 A. Mirkin, C. Liu, A bio-barcode assay for on-chip attomolar-sensitivity protein detection. *Lab Chip* **6**,
963 1293-1299 (2006).
- 964 124. P. S. Waggoner, M. Varshney, H. G. Craighead, Detection of prostate specific antigen with
965 nanomechanical resonators. *Lab Chip* **9**, 3095-3099 (2009).
- 966 125. G. Zheng, X. P. Gao, C. M. Lieber, Frequency domain detection of biomolecules using silicon nanowire
967 biosensors. *Nano Lett.* **10**, 3179-3183 (2010).
- 968 126. S. Schuerle, A. P. Soleimany, T. Yeh, G. M. Anand, M. Haberli, H. E. Fleming, N. Mirkhani, F. Qiu, S.
969 Hauert, X. Wang, B. J. Nelson, S. N. Bhatia, Synthetic and living micropropellers for convection-
970 enhanced nanoparticle transport. *Sci. Adv.* **5**, eaav4803 (2019).
- 971 127. Y. Zhang, L. Zhang, L. Yang, C. I. Vong, K. F. Chan, W. K. K. Wu, T. N. Y. Kwong, N. W. S. Lo, M. Ip,
972 S. H. Wong, J. J. Y. Sung, P. W. Y. Chiu, L. Zhang, Real-time tracking of fluorescent magnetic spore-
973 based microrobots for remote detection of *C. diff* toxins. *Sci. Adv.* **5**, eaau9650 (2019).
- 974 128. J. Wu, S. Balasubramanian, D. Kagan, K. M. Manesh, S. Campuzano, J. Wang, Motion-based DNA
975 detection using catalytic nanomotors. *Nat. Commun.* **1**, 36 (2010).
- 976 129. B. Esteban-Fernandez de Avila, A. Martin, F. Soto, M. A. Lopez-Ramirez, S. Campuzano, G. M. Vasquez-
977 Machado, W. Gao, L. Zhang, J. Wang, Single cell real-time miRNAs sensing based on nanomotors. *ACS*
978 *Nano* **9**, 6756-6764 (2015).
- 979
980
981
982
983
984
985
986
987
988
989

990 **Acknowledgments**

991 X. Y. and Q. Z. are indebted to Li Zhang (The Chinese University of Hong Kong), Tiantian Xu
992 (Shenzhen Institute of Advanced Technology, Chinese Academy of Sciences), Jiangfan Yu
993 (Chinese University of Hong Kong, Shenzhen), and Dongdong Jin (Harbin Institute of
994 Technology, Shenzhen) for their close collaboration and fruitful discussions on research of algae-
995 inspired microrobots over the past decade. This project was sponsored by the National Natural
996 Science Foundation of China (82001845); Fundamental Research Funds for the Central
997 Universities of China (20720190076); Shenzhen Science and Technology Program
998 (JCYJ20190809163407481, JCYJ20200109113408066); Opening Project of Guangdong
999 Provincial Key Lab of Robotics and Intelligent System (XDHT2019588A); Shenzhen Bay
1000 Laboratory (SZBL2019062801005); the Scientific Research Foundation of Xiang An
1001 Biomedicine Laboratory (2023XAKJ0101001, 2023XAKJ0101014)

1002
1003 **Author contributions:**

1004 Conceptualization: X. Y., Q. Z.

1005 Literature review: Z. L., T. L.

1006 Figure preparation: Z. L., T. L., Q. Z.

1007 Supervision: X. Y., Q. Z.

1008 Writing—original draft: Z. L., T. L.

1009 Writing—review & editing: X. S., Q. Z., X. Y.

1010
1011 **Declaration of interests:** The authors declare no competing interests.

1012
1013 **Figures and Tables**

1014 (attached on following pages)

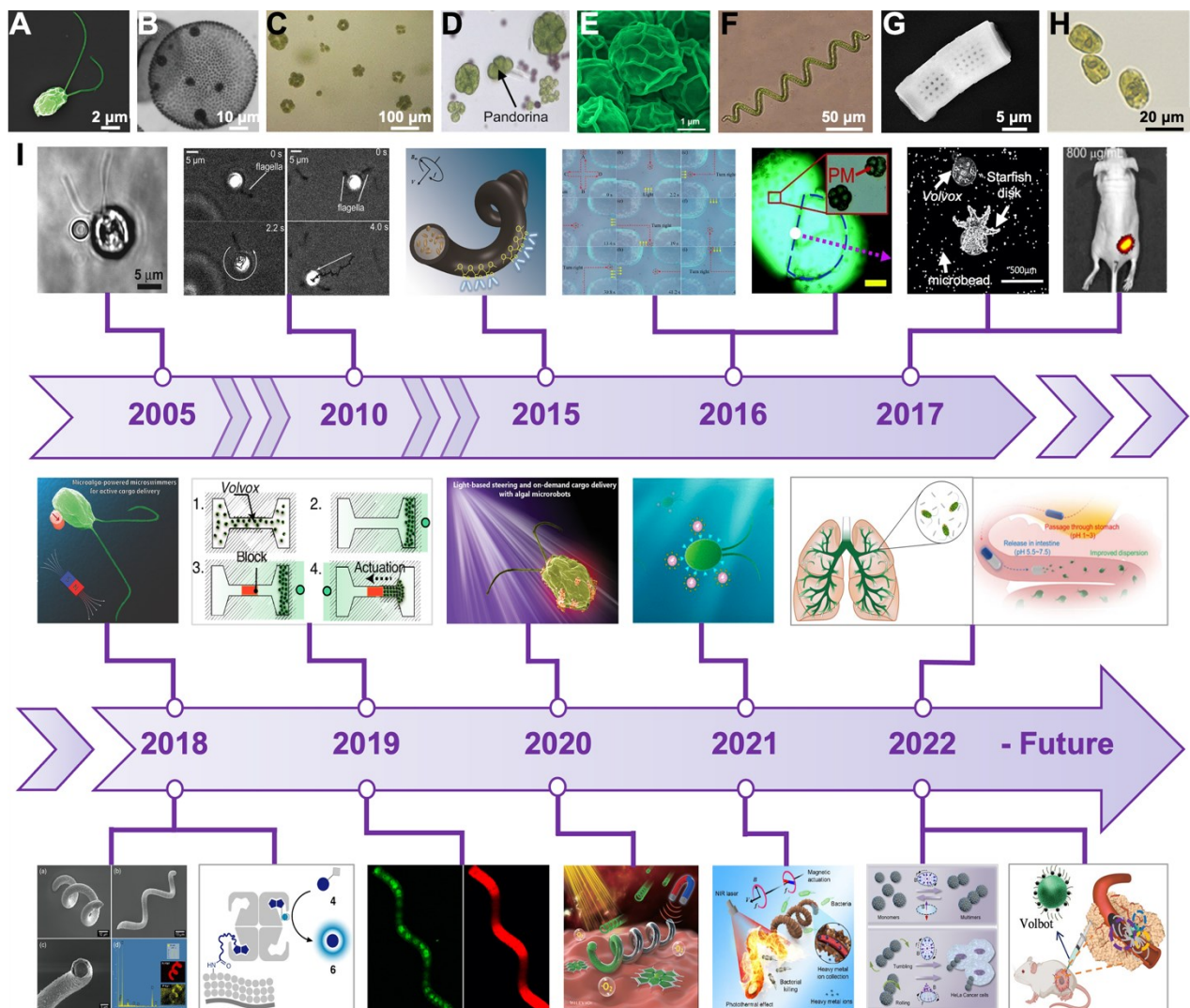
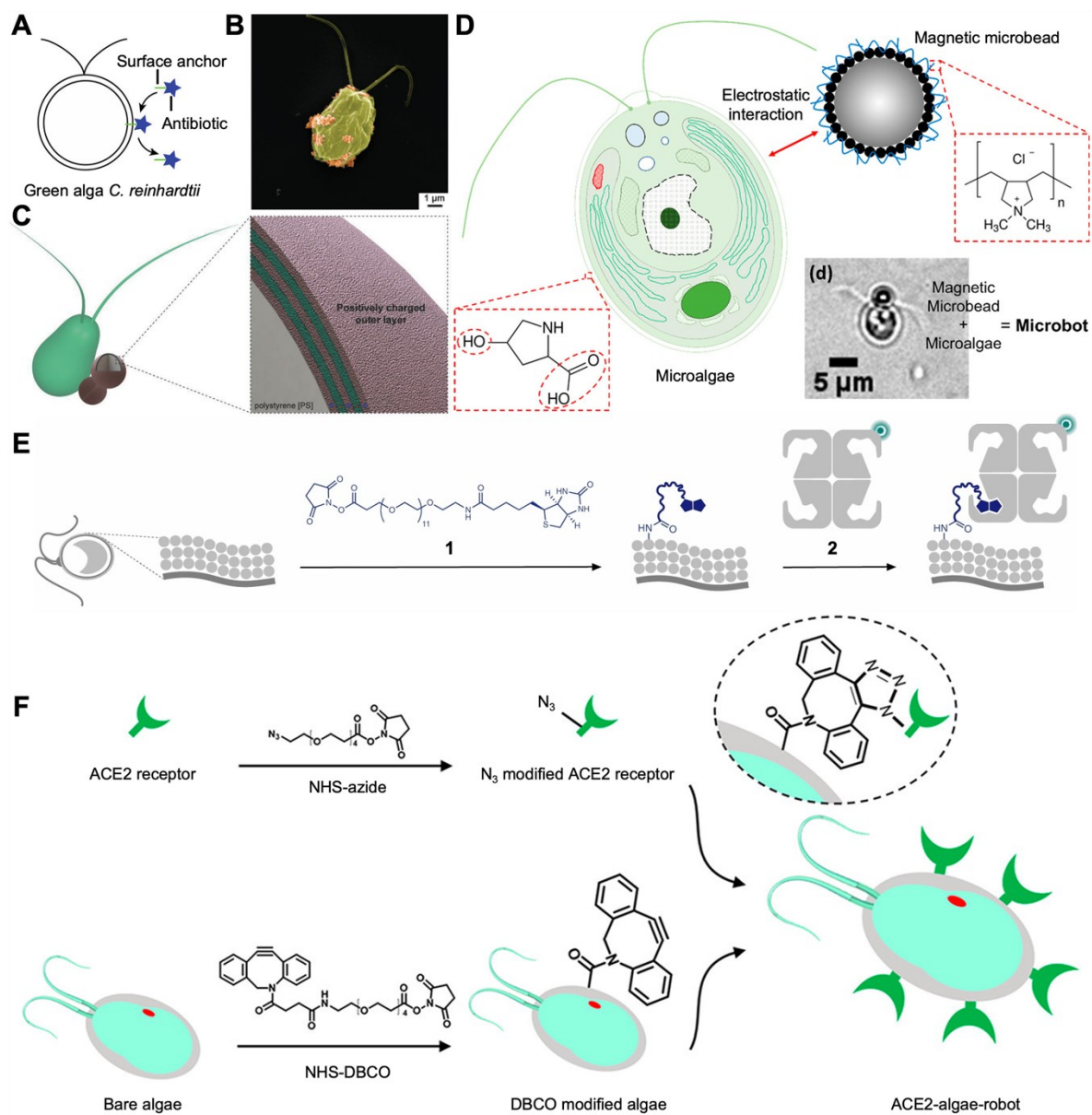
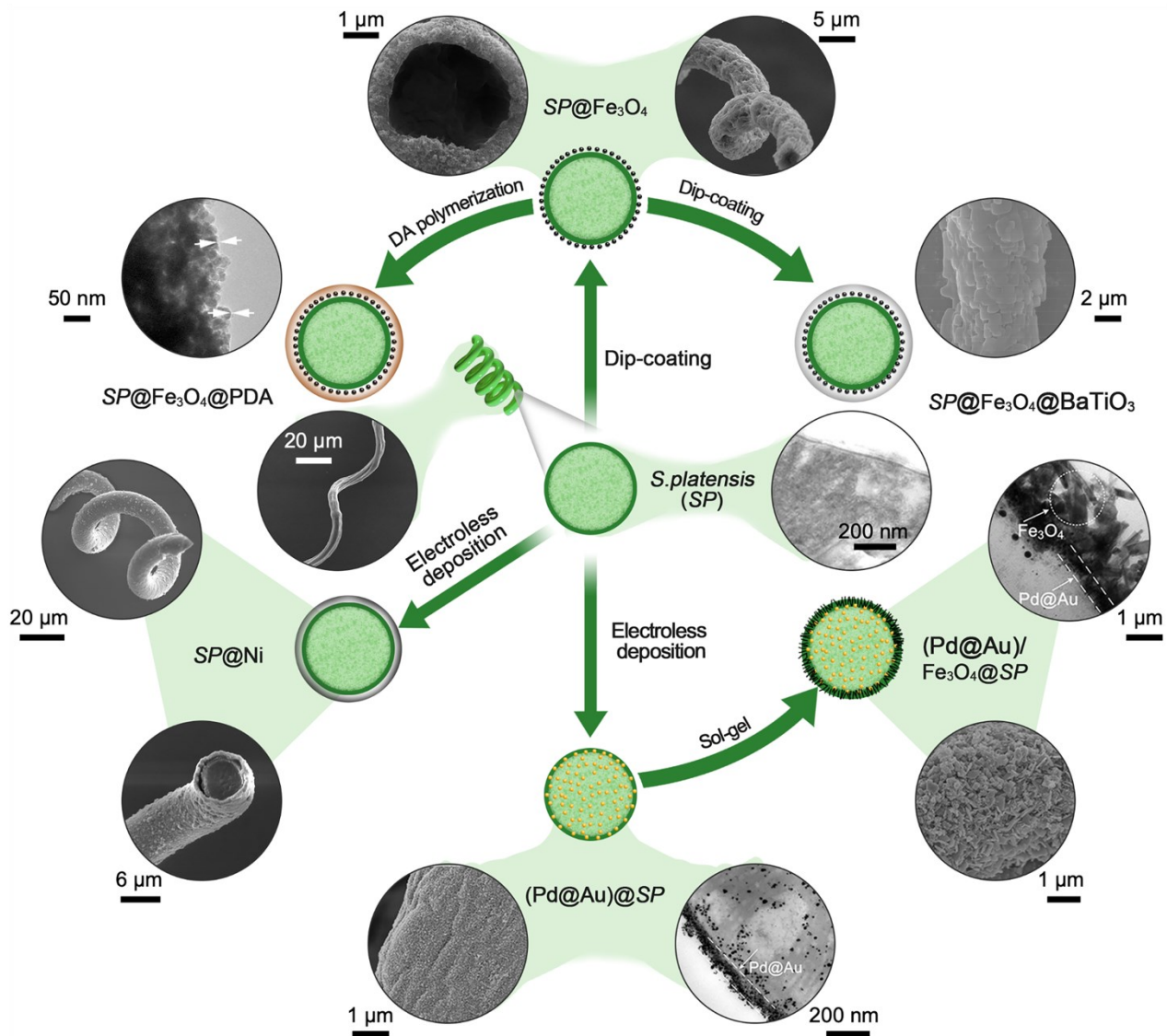


Fig 1. Common microalga species adopted to fabricate microrobots and representative developments of algae-inspired microrobots since 2005. (A) SEM image (pseudocolor) of *Chlamydomonas reinhardtii* (CR);²¹ Copyright, 2020 John Wiley and Sons. (B) Light microscopy image of *Volvox* (VX);²³ Copyright, 2022 John Wiley and Sons. (C) Light microscopy image of *Eudorina elegans* (EE);²⁴ Copyright, 2016 Springer Nature. (D) Light microscopy image of *Pandorina morum* (PM);²⁵ Copyright, 2005 Royal Society of Chemistry. (E) SEM image (pseudocolor) of *Chlorella* (Ch);²⁶ From Qiao et al.²⁶ Reprinted with permission from AAAS. (F) Light microscopy image of *Spirulina platensis* (SP);²⁷ Copyright, 2019 American Chemical Society. (G) SEM image of *Diatom* (DM);²⁸ Copyright, 2020 American Chemical Society. (H) Light microscopy image of *Tetraselmis Subcordiformis* (TS).²⁹ Copyright, 2018 American Chemical Society. (I) Representative AIM developments since its inception in 2005. Controlled microscale cargo transport by CR (2005);²² Copyright, 2005 National Academy of Sciences, U.S.A. Locomotion of flagellated micro-object (2010);³⁰ Reprinted from Mori et al.³⁰, with the permission of AIP Publishing. SP-templated porous hollow swimmer (2015);³¹ Copyright, 2015 John Wiley and Sons. Light-guided motion of robotized CR (2016)²⁴ Copyright, 2016 Springer Nature and Bio-tweezer actuated by PM (2016);²⁵ Copyright, 2005 Royal Society of Chemistry. Manipulation of micro-objects by VX (2017)³² Reprinted from Hatsuzawa et al.³² and *in vivo* imaging of magnetized SP (2017);³³ From Yan et al.³³ Reprinted with permission from AAAS, active cargo delivery by magnetically-guided CR (2018),³⁴ Copyright, 2018 John Wiley and Sons, enhanced propulsion of nickel-plated SP (2018)³⁵ Reprinted from Gong et al.³⁵ and on-cell catalysis & antibacterial therapy by light-guided CR (2018);³⁶ Copyright, 2018 Springer Nature, submillimeter cargo transport by VX (2019)³⁷ Copyright, 2019 MDPI, and cargo delivery & anticancer therapy by magnetic SP (2019);³⁸ Reprinted from Yan et al.³⁸, microoperation & cargo delivery by CR (2020)²¹ Copyright, 2020 John Wiley and Sons, and cell stimulation, anticancer & antibacterial therapy by SP (2020);³⁹ Copyright, 2020 John Wiley and Sons, antibacterial therapy & environment remediation by CR (2021)⁴⁰ Copyright, 2021 American Chemical Society, and detoxification, anticancer & antibacterial treatment by SP (2021);⁴¹ Reprinted from Zheng et al.⁴¹, gastrointestinal drug delivery & acute bacterial pneumonia treatment by CR (2022),^{42,43} Copyright, 2022 Springer Nature and Copyright From Zhang et al.⁴³ Reprinted with permission from AAAS. muscle contraction & anticancer therapy by magnetic Ch (2022)⁴⁴ Copyright, 2022 American Chemical Society and multimodal imaging & therapy by magnetized VX (2022).²³ Copyright, 2022 John Wiley and Sons.



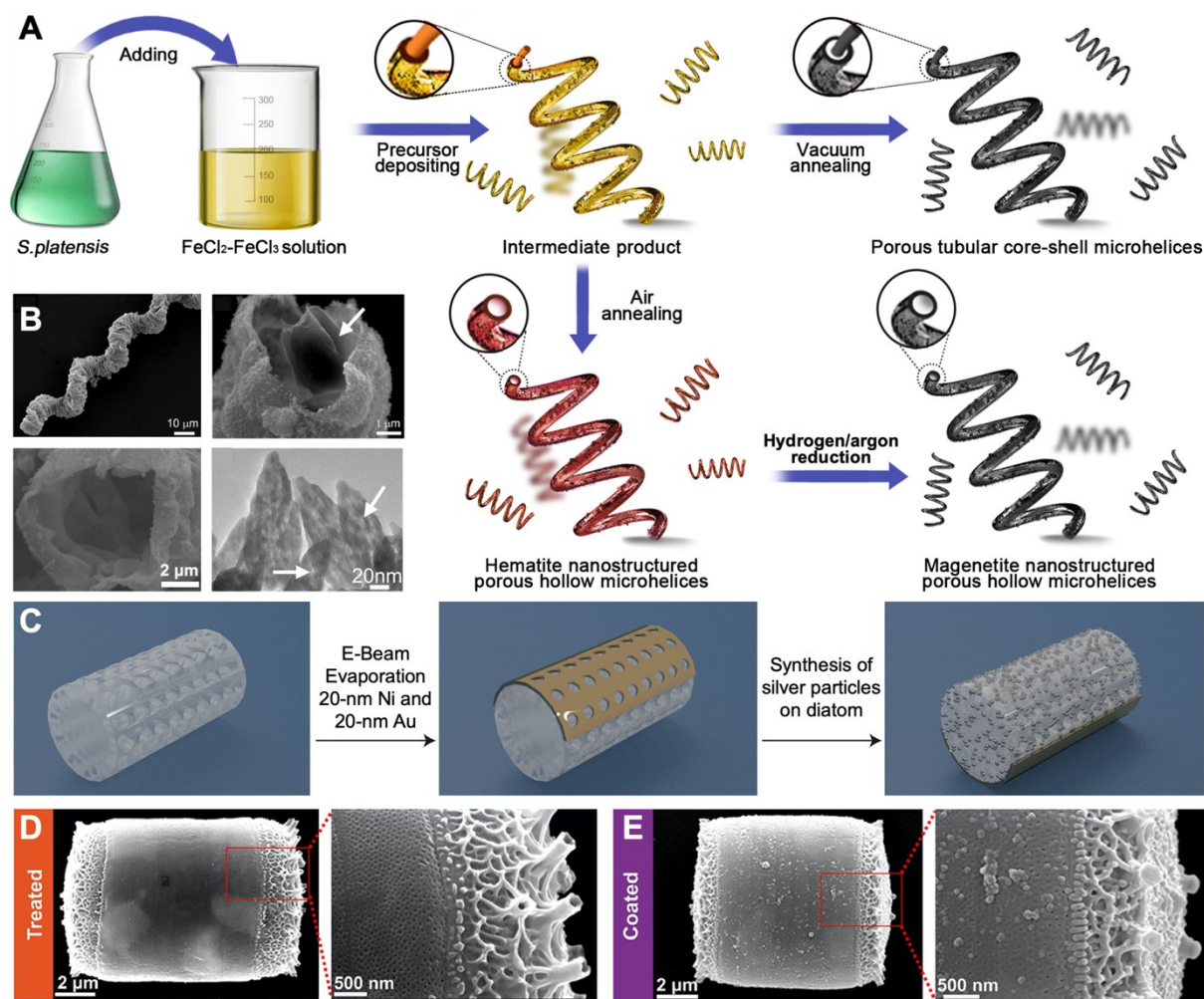
1049
1050
1051
1052
1053
1054
1055
1056
1057

Fig 2. Fabrication methods of MFRs exemplified by CR-based microrobots. (A) Illustration of antibiotic vancomycin and 4-hydroxyproline oligomer reversibly attached to the cell wall of a CR through noncovalent binding.⁵⁹ Copyright, 2018 John Wiley and Sons. (B) Chitosan-coated iron oxide nanoparticles coated on a CR through electrostatic interaction.²¹ Copyright, 2020 John Wiley and Sons. (C) Magnetic PS microparticles attached to a CR with layer-by-layer polyelectrolyte deposition.³⁴ Copyright, 2018 John Wiley and Sons. (D) A magnetic microbead labeled onto CR cell with cationic PDDA modification.⁶¹ Copyright, 2018 American Chemical Society. (E) Surface functionalization of CR with streptavidin binding.³⁶ Copyright, 2018 Springer Nature. (F) Surface modification of CR cells with ACE2 receptor through click chemistry.⁴⁰ Copyright, 2021 American Chemical Society.



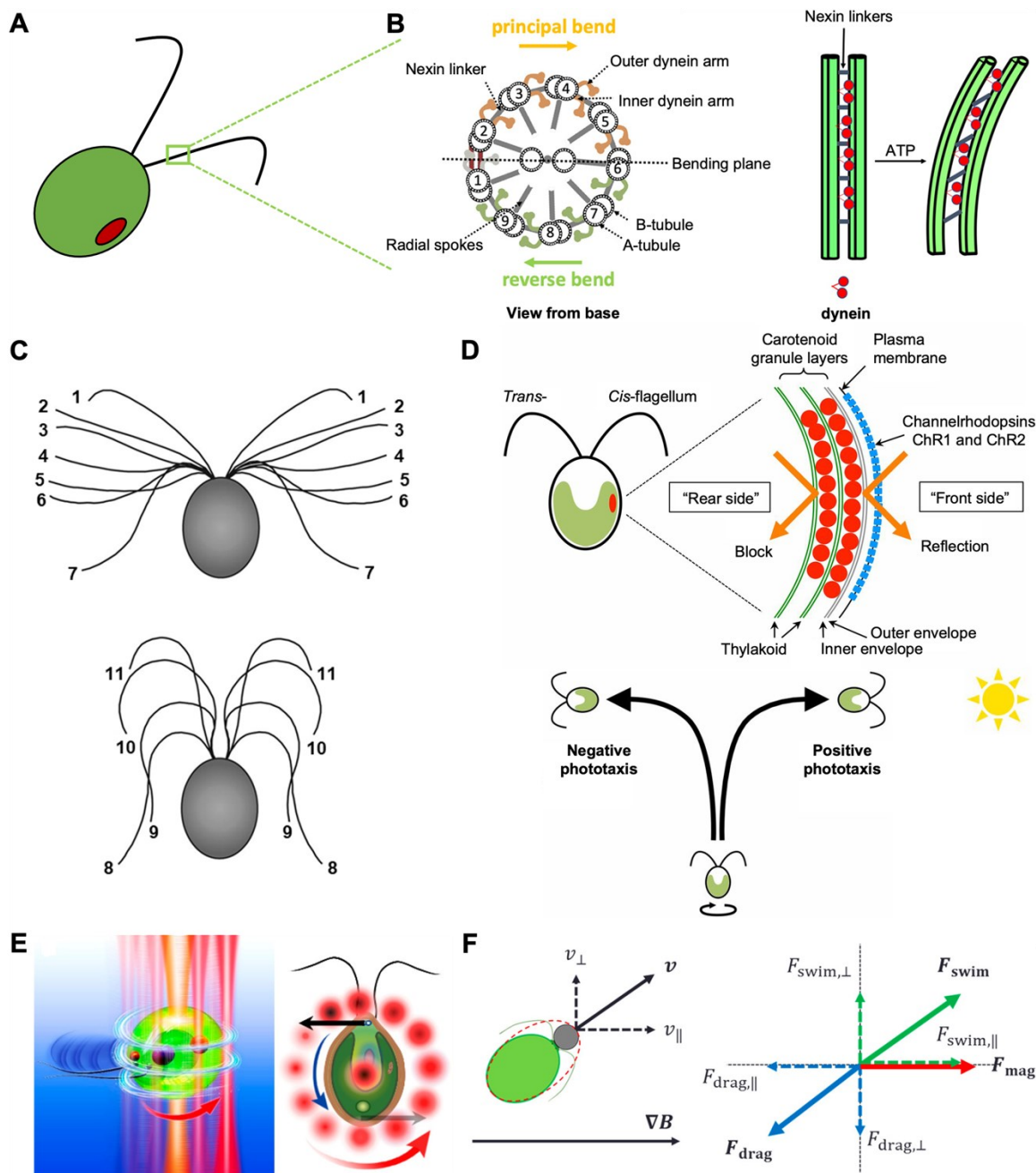
1058
 1059
 1060
 1061
 1062
 1063
 1064
 1065

Fig 3. Fabrication methods of MHRs exemplified by SP-based microrobots. The multi-layer circular schematic demonstrates how various functional materials can be deposited on or incorporated into the SP cells through dip-coating, electroless deposition, sol-gel or polymerization procedures for designated functionalization. $SP@Fe_3O_4$;³³ From Yan et al.³³ Reprinted with permission from AAAS. $SP@Fe_3O_4@PDA$;⁵⁷ Copyright, 2020 American Chemical Society. $SP@Fe_3O_4@BaTiO_3$;⁴⁵ Copyright, 2021 American Chemical Society. $SP@Ni$;³⁵ Reprinted from Gong et al.³⁵ $(Pd@Au)@SP$;²⁷ Copyright, 2019 American Chemical Society. $(Pd@Au)/Fe_3O_4@SP$.²⁷ Copyright, 2019 American Chemical Society.



1066
1067
1068
1069
1070
1071
1072
1073
1074
1075

Fig 4. Fabrication methods of MTRs exemplified by *SP*-based and *Diatom*-based microrobots. (A) Schematic of the procedures for fabricating core-shell⁴¹ and porous-hollow³¹ *SP* MTRs. Copyright, 2015 John Wiley and Sons. **(B)** SEM images of (top row) a core-shell MTR obtained through precursor deposition plus vacuum annealing of the *SP*⁴¹, Reprinted from Zheng et al.⁴¹, and (bottom row) a porous-hollow MTR obtained through precursor deposition, air annealing plus hydrogen/argon reduction of the *SP*.³¹ Copyright, 2015 John Wiley and Sons. The white arrows in the second and fourth panel indicate the carbon core in the middle of the core-shell MTR and the nanoscale mesopores on the shell of the porous-hollow MTR, respectively. **(C)** Schematic of the optoplasmonic MTR fabrication using Diatom frustules.²⁸ Copyright, 2020 American Chemical Society. **(D-E)** Diatom-based MTR fabricated by hydrochloric acid treatment and coating of Fe₃O₄ nanoparticles.⁶⁷ Reprinted from Li et al.⁶⁷



1076
 1077 **Fig 5. Actuation and steering methods of MFRs illustrated by living CR microrobots.** (A) Schematic of
 1078 a *Chlamydomonas* cell. (B) Schematic of the cell's ciliary axonemal cross-section showing how dynein motors convert
 1079 chemical energy from ATP hydrolysis into mechanical work.⁷⁴ Copyright, 2021 American Chemical Society. (C) A
 1080 cartoon illustrating the movement of CR flagella during a beating sequence.²² Copyright, 2005 National Academy of
 1081 Sciences, U.S.A. (D) (top) The eyespot of CR located near the cell equator, consisting of carotenoid granule layers
 1082 (red), photoreceptor proteins, and channelrhodopsins (ChR1 and ChR2; blue). (below) CR adjusts the beating balance
 1083 of its two flagella to exhibit either positive or negative phototaxis.⁷⁷ Copyright, 2016 National Academy of Sciences,
 1084 U.S.A. (E) Schematic of the rotating motion of a CR cell driven by applied optical force.⁹ Copyright, 2020 American
 1085 Chemical Society. (F) Force analysis for a CR attached by a magnetic microbead and placed in a low-gradient magnetic
 1086 field.⁶¹ Copyright, 2018 American Chemical Society.

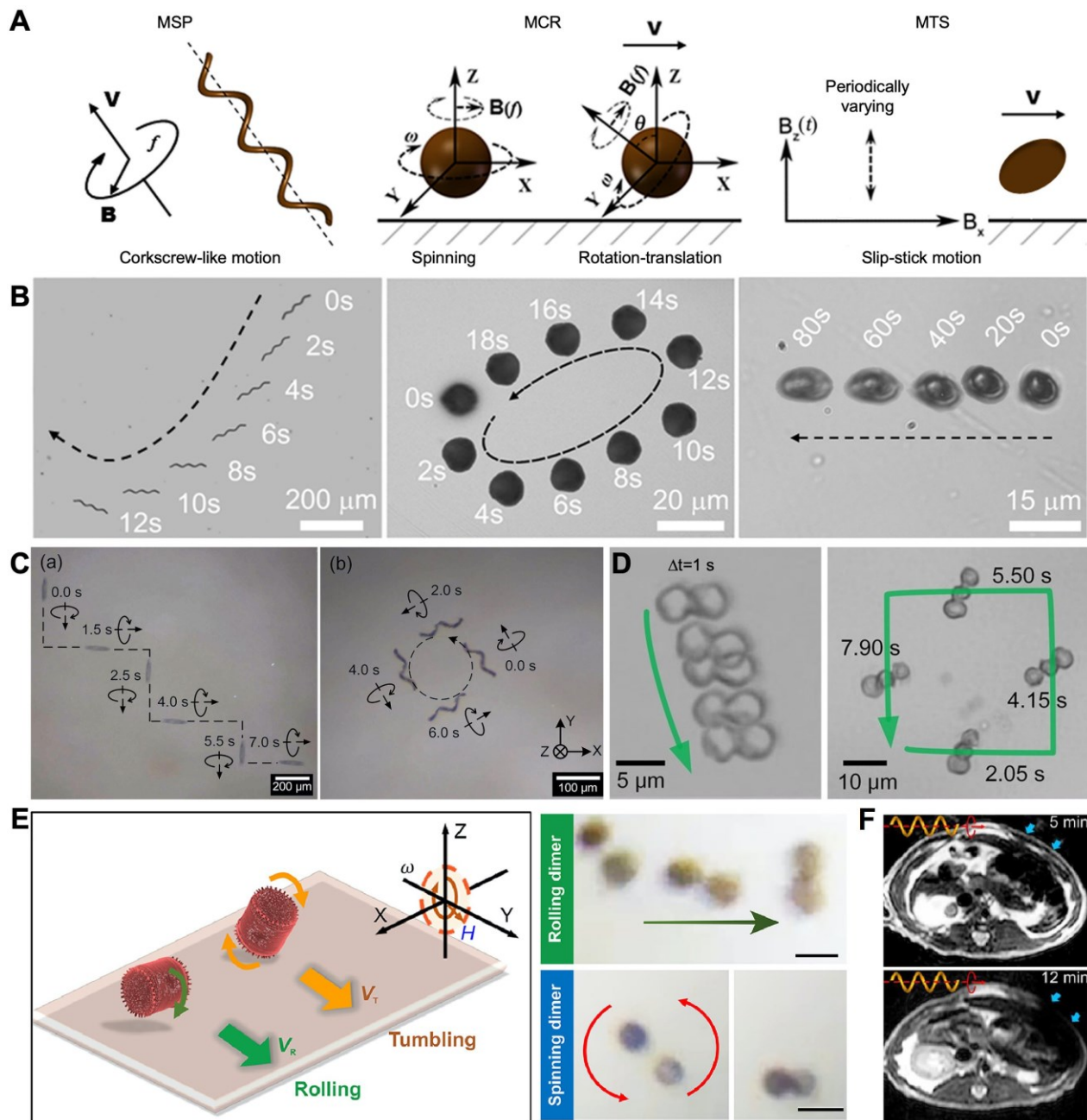
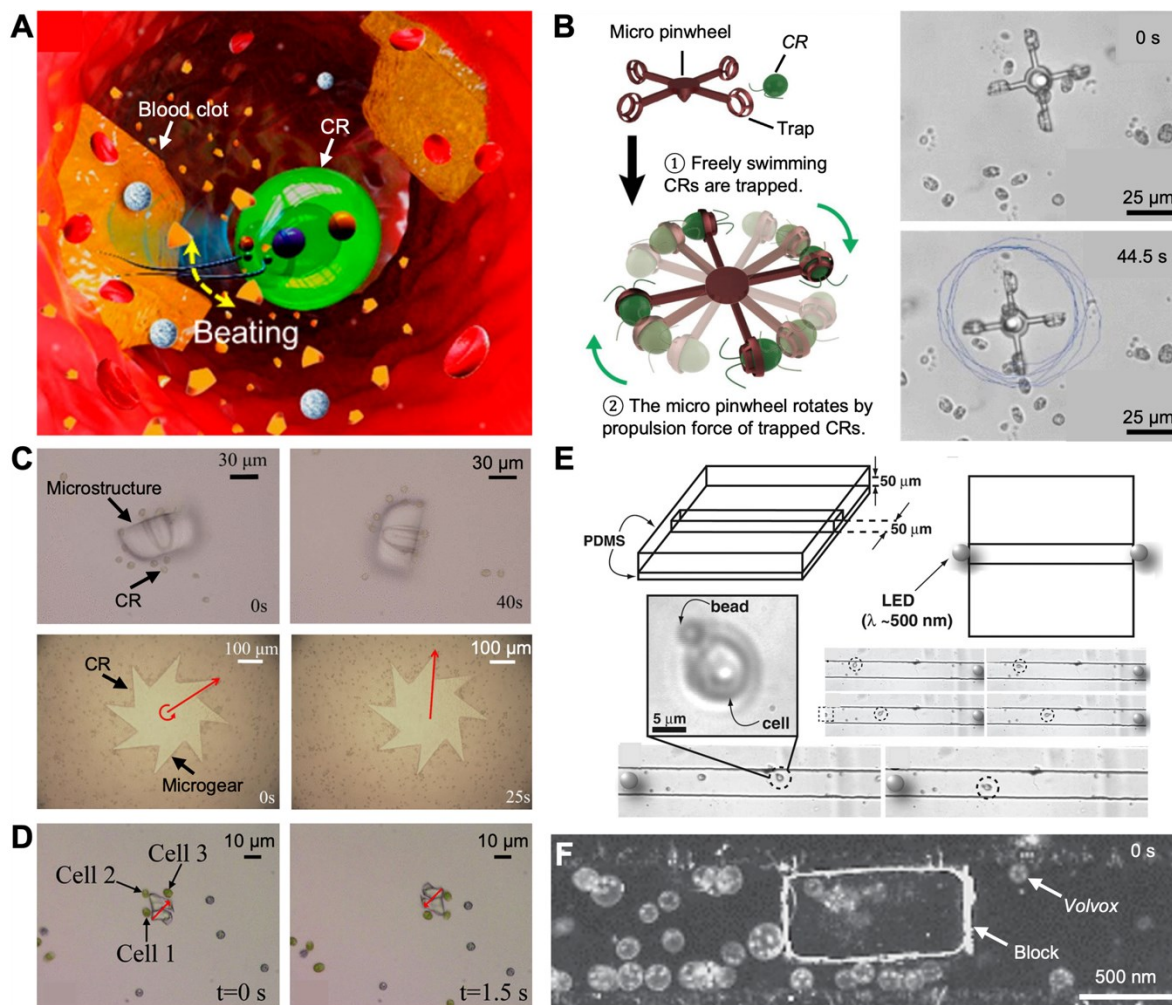
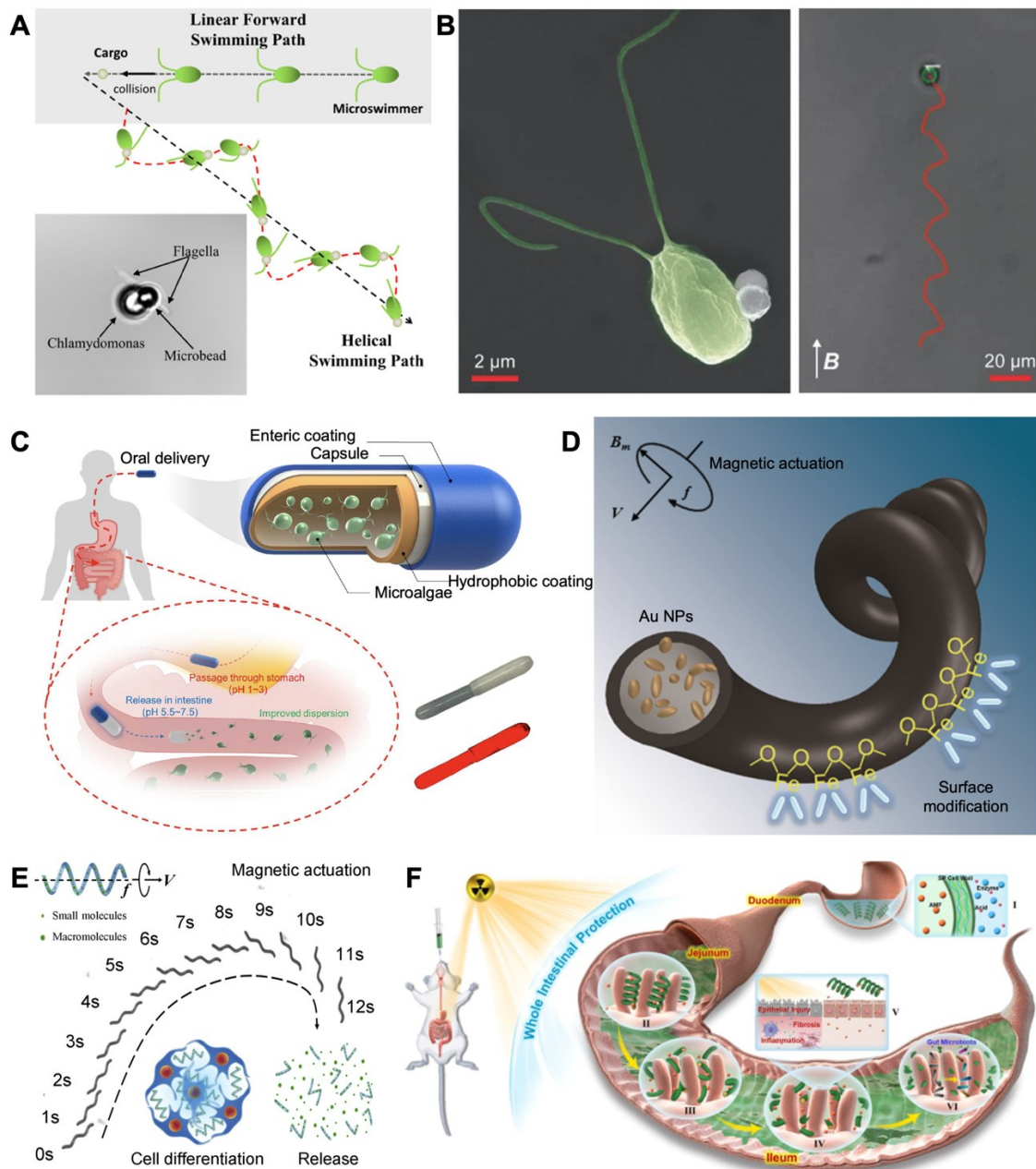


Fig 6. Magnetic actuation and steering of MHRs and MTRs. (A) Schematics of different magnetic actuation strategies for magnetized *SP*, *CR* and *TS*.³³ From Yan et al.³³ Reprinted with permission from AAAS. (B) Time-lapse image sequences showing the controlled locomotion of *SP*, *CR* and *TS* MHRs using the actuation methods in (A).³³ From Yan et al.³³ Reprinted with permission from AAAS. (C) Time-lapse image sequence of the complex maneuver of a *SP* MHR controlled through a rotating magnetic field.³⁵ Reprinted from Gong et al.³⁵ (D) Multiple *Ch* MHRs actuated and steered to perform simple and complex locomotion.⁴⁴ Copyright, 2022 American Chemical Society. (E) Tumbling and rolling motion modes of a Diatom-based MTR under a rotating magnetic field and formation of MTR dimers/trimers.⁶⁷ Reprinted from Li et al.⁶⁷ (F) A swarm of *SP* MHRs remotely actuated in rodent stomach with a rotating magnet and tracked with MR imaging.³³ From Yan et al.³³ Reprinted with permission from AAAS.

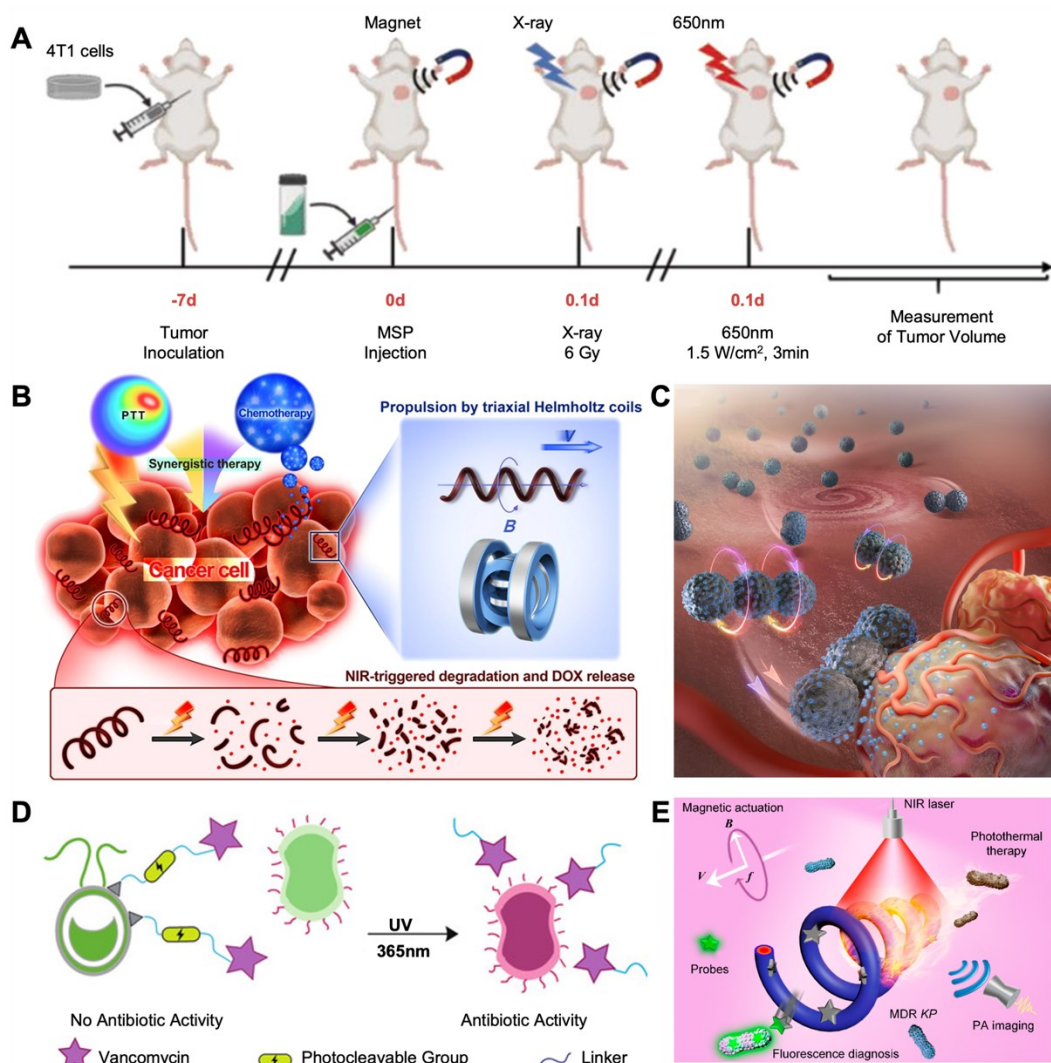


1097
 1098 **Fig 7. Micromanipulation.** (A) Optical force-controlled destruction of bio-aggregates in a capillary-like environment
 1099 through the beating flagella of *CR*-based MFR.⁹ Copyright, 2020 American Chemical Society. (B) Rotation of a micro-
 1100 pinwheel driven by trapped *CR* cells.¹⁰⁶ Copyright, 2021 IEEE. (C) Rotation of micro-objects propelled by randomly
 1101 swimming *CR* cells.¹⁰⁷ Copyright, 2018 IEEE. (D) Controlled assembly and optical-guided cooperative motion of *CR*
 1102 cells for micro-object manipulation.⁵⁸ Copyright, 2005 Royal Society of Chemistry. (E) Microchannel navigation of
 1103 *CR* loading a microbead steered through phototaxis.²² Copyright, 2005 National Academy of Sciences, U.S.A. (F)
 1104 Transport of a submillimeter-sized block in a microchannel by a swarm of *Volvox* through a light irradiation platform.³⁷
 1105 Copyright, 2019 MDPI.



1106
1107
1108
1109
1110
1111
1112
1113
1114

Fig 8. Active delivery. (A) Cargo loading and transport with a freely swimming CR.¹¹⁰ Copyright, 2021 American Chemical Society. (B) Magnetically-assisted delivery with CR attaching a polyelectrolyte-functionalized magnetic cargo.³⁴ Copyright, 2018 John Wiley and Sons. (C) Gastrointestinal tract delivery and retention of therapeutic drugs loaded by CR cells encapsulated in a capsule.⁴³ From Zhang et al.⁴³ Reprinted with permission from AAAS. (D) Loading and release of Au NPs inside SP-based MTR.³¹ Copyright, 2015 John Wiley and Sons. (E) Delivery and release of macromolecules for triggering cell differentiation with SP-based MHR.³⁸ Reprinted from Yan et al.³⁸ (F) Oral delivery of Amifostine-loaded SP MHR for drug accumulation and intestinal protection against cancer radiotherapy.¹¹¹ Copyright, 2010 Nature Publishing Group.



1115
 1116
 1117
 1118
 1119
 1120
 1121
 1122

Fig 9. Anticancer and antibacterial therapy. (A) Combined PDT and RT therapy of solid tumor with *SP*-based magnetic microrobots in a breast tumor model.³⁹ Copyright, 2020 John Wiley and Sons. (B) Synergistic chemophotothermal treatment of cancer cells (EC109 and 769-P) with DOX-loaded *SP* MHRs.²⁷ Copyright, 2019 American Chemical Society. (C) Chemotherapy of HeLa cells with *Ch*-based magnetic microrobots loaded with DOX.⁴⁴ Copyright, 2022 American Chemical Society. (D) Controlled release of antibiotic vancomycin with *CR* cell as living drug carrier.⁶³ Copyright, 2020 John Wiley and Sons. (E) Treatment of pathogenic bacterial infection using a swarm of PDA-coated magnetic *SP* MHRs.⁵⁷ Copyright, 2020 American Chemical Society.

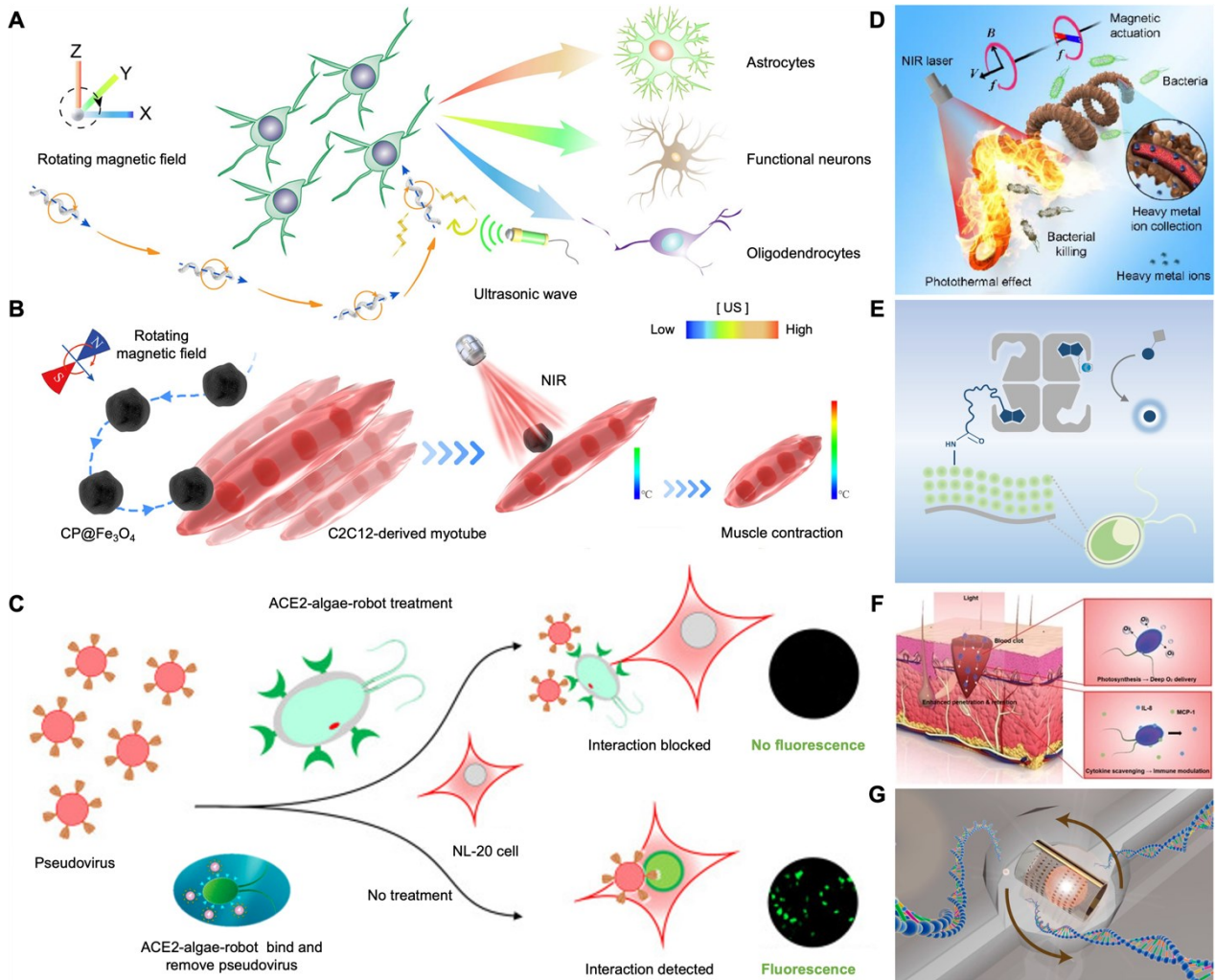


Fig 10. Cell stimulation and other applications. (A) Differentiation of neural stem cells triggered by $SP@Fe_3O_4@BaTiO_3$ MHRs through converting ultrasound waves into electrical signals.⁴⁵ Copyright, 2021 American Chemical Society. (B) Muscle activation through targeted myotube contraction induced by the photothermal effect of *Ch*-based MHR coated with Fe_3O_4 nanoparticles.⁴⁶ Copyright, 2022 American Chemical Society. (C) *Ch*-based MFR for removal of SARS-CoV-2 pseudovirus in water.⁴⁰ Copyright, 2021 American Chemical Society. (D) *SP*-based core-shell MTRs for heavy metal adsorption.⁴¹ Reprinted from Zheng et al.⁴¹ (E) On-cell catalysis through surface functionalization of *CR* with artificial metalloenzyme.³⁶ Copyright, 2018 Springer Nature. (F) Acceleration of wound healing in diabetic mice through enhanced oxygen delivery and cytokine scavenging with *CR*-based microrobots.¹²⁰ Copyright, 2022 John Wiley and Sons. (G) Accelerated DNA enrichment and detection by Diatom-based optoplasmonic micromotor-sensors.²⁸ Copyright, 2020 American Chemical Society.

1147
1148
1149

Table 1. Representative applications of algae-inspired microrobots.

Microrobots	Microalgae	Manufacturing	Functions	Applications	References
Microalgae Flagellated Robots (MFRs)	<i>Chlamydomonas reinhardtii</i> , <i>Eudorina elegans</i> , <i>Pandorina morum</i> , <i>Volvox</i>	Biotin streptavidin binding, electrostatic interaction, click chemistry	Phototaxis/magnetotaxis, photodynamic/photothermal, biocompatibility, degradability, oxygen generation, immunoregulation	Micromanipulation Active drug delivery Anticancer therapy Antibacterial therapy Biological detoxification On-cell enzyme catalysis Wound healing	9, 22, 25, 37, 58, 106, 107 21, 22, 34, 43, 110 23 42, 59, 63 40, 56 36 120
Microalgae Hybrid Robots (MHRs)	<i>Spirulina platensis</i> , <i>Chlorella</i> , <i>Diatom</i> , <i>Chlamydomonas reinhardtii</i> , <i>Tetraselmis subcordiformis</i>	Dip-coating, sol-gel, electroless deposition, surface polymerization, electrostatic interaction	Drug loading/release, off-on fluorescence sensing, enhanced photothermal, selective cytotoxicity, tunable biodegradability, piezoelectric effect, opto-hydrodynamic effect	Active drug delivery Anticancer therapy Antibacterial therapy Disease diagnosis Cell stimulation Biological detoxification	38, 111 27, 33, 39, 44 57, 65 33, 57 45, 46, 66 121
Microalgae Templated Robots (MTRs)	<i>Spirulina platensis</i> , <i>Diatom</i>	Biomineralization, annealing treatment, physical vapor deposition, electrostatic interaction	High payload capacity, photothermal effect, remote biosensing, heavy metal ion adsorption	Active drug delivery Antibacterial therapy Biological detoxification Biomolecule detection	31, 67 41 41 28

1150